Analytical solution for vibration and buckling of functionally graded sandwich beams using various quasi-3D theories

Adelaja I. Osofero[a], Thuc P. Vo[a,*], Trung-Kien Nguyen[b], Jaehong Lee[c]

[a] *Faculty of Engineering and Environment, Northumbria University, Newcastle upon Tyne, NE1 8ST, UK.*
[b] *Faculty of Civil Engineering and Applied Mechanics, University of Technical Education Ho Chi Minh City, 1 Vo Van Ngan Street, Thu Duc District, Ho Chi Minh City, Vietnam*
[c] *Department of Architectural Engineering, Sejong University 98 Kunja Dong, Kwangjin Ku, Seoul 143-747, Korea.*

Abstract

This paper presents analytical solution for vibration and buckling of functionally graded (FG) sandwich beams using various quasi-3D theories, which consider effects of both shear and normal deformation. Sandwich beams with FG skins-homogeneous core and homogeneous skins-FG core are considered. By using the Hamilton's principle, governing equations of motion are derived. Analytical solution is presented, and the obtained results by various quasi-3D theories are compared with each other and with the available solutions in the literature. The effects of normal strain, power-law indexes, skin-core-skin thickness and slenderness ratios on vibration and buckling behaviour of sandwich beams are investigated.

Keywords: Functionally graded sandwich beams; vibration; buckling; quasi-3D theory

1. Introduction

Sandwich structures have been widely used in automotive, marine and aerospace industries where strong, stiff, and lightweight structures are required. Conventional sandwich structures, composed of a soft core bonded to two thin and stiff skins, exhibit delamination problems at the interfaces between layers. To overcome this problem, functionally graded (FG) sandwich structures are proposed due to the gradual variation of material properties through their thickness. They commonly exist in two types: FG skins-homogeneous core and homogeneous skins-FG core. With the wide application of sandwich structures, understanding their vibration and buckling response using more accurate theories becomes an important task. Due to shear deformation effects, the first-order shear deformation theory and higher-order shear deformation theories are usually used in FG sandwich plates. First-order shear

*Corresponding author, tel.: +44 191 243 7856
Email address: thuc.vo@northumbria.ac.uk (Thuc P. Vo)

deformation theory ([1], [2]) assumes the constant shear strain distribution through the thickness and thus, needs a shear correction factor in order to satisfy the stress-free boundary conditions on the top and bottom surfaces of the plate. To avoid the use of a shear correction factor, various higher-order shear deformation theories have been proposed ([3]-[11]). In these theories above, the transverse displacement is considered to be independent of thickness coordinates, which means that the effect of thickness stretching or normal deformation is neglected. This effect in FG plates was investigated by Carrera et al. [12] using finite element approximations. The various higher-order shear and normal deformable theories, which are also called quasi-3D theories, were proposed to analyse FG sandwich plates by many researchers ([13]-[19]). However, there are limited papers using these theories for FG sandwich beams. Carrera et al. [20] developed Carrera Unified Formulation, which included the stretching effect, using various refined theories for FG beams. This formulation was latter on extended for the free vibration of FG sandwich beams [21]. Based on the third-order beam theory, Vo et al. [22] developed a simple quasi-3D theory for vibration and buckling of FG sandwich beams using finite element model.

In this paper, various higher-order shear and normal deformation theories are developed for the vibration and buckling analysis of FG sandwich beams. The effects of shear and normal deformation are included. Analytical solution is obtained for simply-supported sandwich beams. Numerical studies are carried out and the obtained results by various quasi-3D theories, which are based on the sinusoidal beam theory (SBT), hyperbolic beam theory (HBT), and exponential beam theory (EBT), are compared with each other and with the available solutions in the literature. The effects of normal strain, power-law indexes, skin-core-skin thickness and slenderness ratios on vibration and buckling behaviour of sandwich beams are investigated.

2. FG sandwich beams

Consider a FG sandwich beam with length L and rectangular cross-section $b \times h$, with b being the width and h being the height. It should be noted that FG materials considered here work in elevated or lowered temperature conditions. Besides, changes of material properties caused by temperature and thermal expansions are neglected. For simplicity, Poisson's ratio ν, is assumed to be constant. The effective material properties, such as Young's modulus E and mass density ρ, are assumed to vary continuously through the beam depth by a power-law distribution [23] given as :

$$P(z) = (P_c - P_m)V_c + P_m \tag{1}$$

where subscripts m and c represent the metallic and ceramic constituents, V_c is the volume fraction of the ceramic phase of the beam. Two different types of FG sandwich beam are studied:

2.1. Type A: sandwich beam with FG skins and homogeneous core

The core is fully ceramic and skins are graded from metal to ceramic (Fig. 1a). The volume fraction of the ceramic phase is obtained by([3],[4]):

$$\begin{cases} V_c = \left(\frac{z-h_o}{h_1-h_0}\right)^k, & z \in [-h/2, h_1] \quad \text{(bottom skin)} \\ V_c = 1, & z \in [h_1, h_2] \quad \text{(core)} \\ V_c = \left(\frac{z-h_3}{h_2-h_3}\right)^k, & z \in [h_2, h/2] \quad \text{(top skin)} \end{cases} \tag{2}$$

where k is the power-law index.

2.2. Type B: sandwich beam with homogeneous skins and FG core

The bottom skin is fully metal and the top skin is fully ceramic, while, the core layer is composed of a FG material (Fig. 1b). The volume fraction of the ceramic phase is obtained by [15]:

$$\begin{cases} V_c = 0, & z \in [-h/2, h_1] \quad \text{(bottom skin)} \\ V_c = \left(\frac{z-h_1}{h_2-h_1}\right)^k, & z \in [h_1, h_2] \quad \text{(core)} \\ V_c = 1, & z \in [h_2, h/2] \quad \text{(top skin)} \end{cases} \tag{3}$$

2.3. Constitutive Equations

The constitutive relations of a FG sandwich beam can be written as:

$$\begin{Bmatrix} \sigma_x \\ \sigma_z \\ \sigma_{xz} \end{Bmatrix} = \begin{bmatrix} \bar{C}^*_{11} & \bar{C}^*_{13} & 0 \\ \bar{C}^*_{13} & \bar{C}^*_{11} & 0 \\ 0 & 0 & C_{55} \end{bmatrix} \begin{Bmatrix} \epsilon_x \\ \epsilon_z \\ \gamma_{xz} \end{Bmatrix} \tag{4}$$

where

$$\bar{C}^*_{11} = \bar{C}_{11} - \frac{\bar{C}^2_{12}}{\bar{C}_{22}} = \frac{E(z)}{1-\nu^2} \tag{5a}$$

$$\bar{C}^*_{13} = \bar{C}_{13} - \frac{\bar{C}_{12}\bar{C}_{23}}{\bar{C}_{22}} = \frac{E(z)\nu}{1-\nu^2} \tag{5b}$$

$$C_{55} = \frac{E(z)}{2(1+\nu)} \tag{5c}$$

3. Theoretical Formulation

3.1. Kinematics

The present theory is based on the following displacement field:

$$U(x,z,t) = u(x,t) - zw_b'(x,t) - f(z)w_s'(x,t) \tag{6a}$$

$$W(x,z,t) = w_b(x,t) + w_s(x,t) + g(z)w_z(x,t) \tag{6b}$$

where u, w_b, w_s and w_z are four unknown displacements of mid-plane of the beam. Shape functions $f(z)$ and $g(z) = 1 - \frac{df(z)}{dz}$ are used to determine the distribution of the strain through the beam depth. They are chosen to satisfy the stress-free boundary conditions on the top and bottom surfaces of the beam, thus a shear correction factor is not required. Although many shape functions are available, only the sinusoidal beam theory (SBT) based on Touratier [24], hyperbolic beam theory (HBT) based on Soldatos [25] and exponential beam theory (EBT) based on Karama [26] are considered in this study:

$$f(z) = z - \frac{h}{\pi}\sin(\frac{\pi z}{h}) \quad \text{for SBT} \tag{7a}$$

$$f(z) = z - h\sinh(\frac{z}{h}) + z\cosh(\frac{1}{2}) \quad \text{for HBT} \tag{7b}$$

$$f(z) = z - ze^{-2(\frac{z}{h})^2} \quad \text{for EBT} \tag{7c}$$

The strains associated with the displacement field in Eq. (6) are as follows:

$$\epsilon_x = \frac{\partial U}{\partial x} = u' - zw_b'' - fw_s'' \tag{8a}$$

$$\epsilon_z = \frac{\partial W}{\partial z} = g'w_z \tag{8b}$$

$$\gamma_{xz} = \frac{\partial W}{\partial x} + \frac{\partial U}{\partial z} = g(w_s' + w_z') \tag{8c}$$

3.2. Variational Formulation

The variation of the strain energy can be stated as:

$$\begin{aligned}\delta\mathcal{U} &= \int_0^l \int_0^b \left[\int_{-h/2}^{h/2} (\sigma_x \delta\epsilon_x + \sigma_{xz}\delta\gamma_{xz} + \sigma_z g'\delta w_z)dz \right] dydx \\ &= \int_0^l \left[N_x\delta u' - M_x^b\delta w_b'' - M_x^s\delta w_s'' + Q_{xz}(\delta w_s' + \delta w_z') + R_z\delta w_z \right])dx \end{aligned} \tag{9}$$

where $N_x, M_x^b, M_x^s, Q_{xz}$ and R_z are the stress resultants, defined as:

$$N_x = \int_{-h/2}^{h/2} \sigma_x b dz \tag{10a}$$

$$M_x^b = \int_{-h/2}^{h/2} \sigma_x z b dz \tag{10b}$$

$$M_x^s = \int_{-h/2}^{h/2} \sigma_x f b dz \tag{10c}$$

$$Q_{xz} = \int_{-h/2}^{h/2} \sigma_{xz} g b dz \tag{10d}$$

$$R_z = \int_{-h/2}^{h/2} \sigma_z g' b dz \tag{10e}$$

The variation of the potential energy by the axial force P_0 can be written as:

$$\delta\mathcal{V} = -\int_0^l P_0 \Big[\delta w_b'(w_b' + w_s') + \delta w_s'(w_b' + w_s')\Big] dx \tag{11}$$

The variation of the kinetic energy can be expressed as:

$$\begin{aligned}
\delta\mathcal{K} &= \int_0^l \int_0^b \left[\int_{-h/2}^{h/2} \rho(\dot{U}\delta\dot{U} + \dot{W}\delta\dot{W}) dz\right] dy dx \\
&= \int_0^l \Big[\delta\dot{u}(m_0\dot{u} - m_1\dot{w_b}' - m_f\dot{w_s}') + \delta\dot{w_b}[m_0(\dot{w_b} + \dot{w_s}) + m_g\dot{w_z}] + \delta\dot{w_b}'(-m_1\dot{u} + m_2\dot{w_b}' + m_{fz}\dot{w_s}') \\
&+ \delta\dot{w_s}[m_0(\dot{w_b} + \dot{w_s}) + m_g\dot{w_z}] + \delta\dot{w_s}'(-m_f\dot{u} + m_{fz}\dot{w_b}' + m_{f^2}\dot{w_s}') \\
&+ \delta\dot{w_z}[m_g(\dot{w_b} + \dot{w_s}) + m_{g^2}\dot{w_z}]\Big] dx
\end{aligned} \tag{12}$$

where

$$(m_0, m_1, m_2) = \int_{-h/2}^{h/2} \rho(1, z, z^2) b dz \tag{13a}$$

$$(m_f, m_{fz}, m_{f^2}) = \int_{-h/2}^{h/2} \rho(f, fz, f^2) b dz \tag{13b}$$

$$(m_g, m_{g^2}) = \int_{-h/2}^{h/2} \rho(g, g^2) b dz \tag{13c}$$

By using Hamilton's principle, the following weak statement is obtained:

$$\int_{t_1}^{t_2} (\delta\mathcal{K} - \delta\mathcal{U} - \delta\mathcal{V}) dt = 0 \tag{14a}$$

$$\begin{aligned}
\int_{t_1}^{t_2} \int_0^l \Big[&\delta\dot{u}(m_0\dot{u} - m_1\dot{w_b}' - m_f\dot{w_s}') + \delta\dot{w_b}[m_0(\dot{w_b} + \dot{w_s}) + m_g\dot{w_z}] \\
&+\delta\dot{w_b}'(-m_1\dot{u} + m_2\dot{w_b}' + m_{fz}\dot{w_s}') + \delta\dot{w_s}[m_0(\dot{w_b} + \dot{w_s}) + m_g\dot{w_z}] \\
&+\delta\dot{w_s}'(-m_f\dot{u} + m_{fz}\dot{w_b}' + m_{f^2}\dot{w_s}') + \delta\dot{w_z}[m_g(\dot{w_b} + \dot{w_s}) + m_{g^2}\dot{w_z}] \\
&+P_0\Big[\delta w_b'(w_b' + w_s') + \delta w_s'(w_b' + w_s')\Big] \\
&-N_x\delta u' + M_x^b\delta w_b'' + M_x^s\delta w_s'' - Q_{xz}\delta w_s' - R_z\delta w_z\Big] dx dt = 0
\end{aligned} \tag{14b}$$

3.3. Governing Equations

Integrating Eq. (14) by parts and collecting the coefficients of $\delta u, \delta w_b$, δw_s and δw_z, the governing equations of motion can be obtained:

$$
\begin{aligned}
N_x' &= m_0\ddot{u} - m_1\ddot{w}_b{}' - m_f\ddot{w}_s{}' && \text{(15a)}\\
M_x^{b\prime\prime} - P_0(w_b'' + w_s'') &= m_0(\ddot{w}_b + \ddot{w}_s) + m_1\ddot{u}' - m_2\ddot{w}_b{}'' - m_{fz}\ddot{w}_s{}'' + m_g\ddot{w}_z && \text{(15b)}\\
M_x^{s\prime\prime} + Q_{xz}' - P_0(w_b'' + w_s'') &= m_0(\ddot{w}_b + \ddot{w}_s) + m_f\ddot{u}' - m_{fz}\ddot{w}_b{}'' - m_{f^2}\ddot{w}_s{}'' + m_g\ddot{w}_z && \text{(15c)}\\
Q_{xz}' - R_z &= m_g(\ddot{w}_b + \ddot{w}_s) + m_{g^2}\ddot{w}_z && \text{(15d)}
\end{aligned}
$$

Substituting Eqs. (4) and (8) into Eq. (10), the stress resultants can be expressed in term of displacements:

$$
\begin{Bmatrix} N_x \\ M_x^b \\ M_x^s \\ R_z \\ Q_{xz} \end{Bmatrix} = \begin{bmatrix} A & B & B_s & X & 0 \\ & D & D_s & Y & 0 \\ & & H & Y_s & 0 \\ & & & Z & 0 \\ sym. & & & & A_s \end{bmatrix} \begin{Bmatrix} u' \\ -w_b'' \\ -w_s'' \\ w_z \\ w_s' + w_z' \end{Bmatrix} \qquad \text{(16)}
$$

where

$$
\begin{aligned}
(A, B, B_s, D, D_s, H, Z) &= \int_{-h/2}^{h/2} \bar{C}_{11}^*(1, z, f, z^2, fz, f^2, g'^2) b dz && \text{(17a)}\\
A_s &= \int_{-h/2}^{h/2} C_{55} g^2 b dz && \text{(17b)}\\
(X, Y, Y_s) &= \int_{-h/2}^{h/2} \bar{C}_{13}^* g'(1, z, f) b dz && \text{(17c)}
\end{aligned}
$$

By substituting Eq. (16) into Eq. (15), the explicit form of the governing equations of motion can be expressed:

$$
\begin{aligned}
Au'' - Bw_b''' - B_s w_s''' + Xw_z' &= m_0\ddot{u} - m_1\ddot{w}_b{}' - m_f\ddot{w}_s{}' && \text{(18a)}\\
Bu''' - Dw_b^{iv} - D_s w_s^{iv} + Yw_z'' - P_0(w_b'' + w_s'') &= m_1\ddot{u}' + m_0(\ddot{w}_b + \ddot{w}_s) - m_2\ddot{w}_b{}''\\
&\quad - m_{fz}\ddot{w}_s{}'' + m_g\ddot{w}_z && \text{(18b)}\\
B_s u''' - D_s w_b^{iv} - Hw_s^{iv} + A_s w_s'' + (A_s + Y_s)w_z'' - P_0(w_b'' + w_s'') &= m_f\ddot{u}' + m_0(\ddot{w}_b + \ddot{w}_s) - m_{fz}\ddot{w}_b{}''\\
&\quad - m_{f^2}\ddot{w}_s{}'' + m_g\ddot{w}_z && \text{(18c)}\\
-Xu' + Yw_b'' + (A_s + Y_s)w_s'' + A_s w_z'' - Zw_z &= m_g(\ddot{w}_b + \ddot{w}_s) + m_{g^2}\ddot{w}_z && \text{(18d)}
\end{aligned}
$$

4. Analytical solutions

The Navier solution procedure is used to determine the analytical solutions for a simply-supported sandwich beam. The solution is assumed to be of the form:

$$u(x,t) = \sum_{n=1}^{\infty} U_n \cos\alpha x\, e^{i\omega t} \tag{19a}$$

$$w_b(x,t) = \sum_{n=1}^{\infty} W_{bn} \sin\alpha x\, e^{i\omega t} \tag{19b}$$

$$w_s(x,t) = \sum_{n=1}^{\infty} W_{sn} \sin\alpha x\, e^{i\omega t} \tag{19c}$$

$$w_s(x,t) = \sum_{n=1}^{\infty} W_{zn} \sin\alpha x\, e^{i\omega t} \tag{19d}$$

where $\alpha = n\pi/L$ and U_n, W_{bn}, W_{sn} and W_{zn} are the coefficients.

By substituting Eq. (19) into Eq. (18), the analytical solution can be obtained from the following equations:

$$\left(\begin{bmatrix} K_{11} & K_{12} & K_{13} & K_{14} \\ & K_{22}-P_0\alpha^2 & K_{23}-P_0\alpha^2 & K_{24} \\ & & K_{33}-P_0\alpha^2 & K_{34} \\ \text{sym.} & & & K_{44} \end{bmatrix} - \omega^2 \begin{bmatrix} M_{11} & M_{12} & M_{13} & 0 \\ & M_{22} & M_{23} & M_{24} \\ & & M_{33} & M_{34} \\ \text{sym.} & & & M_{44} \end{bmatrix} \right) \begin{Bmatrix} U_n \\ W_{bn} \\ W_{sn} \\ W_{zn} \end{Bmatrix} = \begin{Bmatrix} 0 \\ 0 \\ 0 \\ 0 \end{Bmatrix} \tag{20}$$

where

$$K_{11} = A\alpha^2; \quad K_{12} = -B\alpha^3; \quad K_{13} = -B_s\alpha^3; \quad K_{14} = -X\alpha \tag{21a}$$

$$K_{22} = D\alpha^4; \quad K_{23} = D_s\alpha^4; \quad K_{24} = Y\alpha^2 \tag{21b}$$

$$K_{33} = A_s\alpha^2 + H\alpha^4; \quad K_{34} = (A_s + Y_s)\alpha^2; \quad K_{44} = A_s\alpha^2 + Z \tag{21c}$$

$$M_{11} = m_0; \quad M_{12} = -m_1\alpha; \quad M_{13} = -m_f\alpha \tag{21d}$$

$$M_{22} = m_0 + m_2\alpha^2; \quad M_{23} = m_0 + m_{fz}\alpha^2; \quad M_{24} = m_g \tag{21e}$$

$$M_{33} = m_0 + m_{f^2}\alpha^2; \quad M_{34} = m_g; \quad M_{44} = m_{g^2} \tag{21f}$$

5. Numerical Examples

The accuracy of the present theory is hereby demonstrated by various numerical examples discussed in this section. FG sandwich beams made of Aluminum as metal (Al: $E_m = 70\text{GPa}, \nu_m = 0.3, \rho_m =$

2702kg/m^3) and Alumina as ceramic (Al_2O_3: $E_c = 380\text{GPa}, \nu_c = 0.3, \rho_c = 3960\text{kg/m}^3$) with two slenderness ratios, $L/h = 5$ and 20, are considered. The following dimensionless natural frequencies and critical buckling loads are used:

$$\overline{\omega} = \frac{\omega L^2}{h}\sqrt{\frac{\rho_m}{E_m}} \tag{22a}$$

$$\overline{P}_{cr} = P_{cr}\frac{12L^2}{E_m h^3} \tag{22b}$$

Tables 1-8 show the fundamental natural frequencies and critical buckling loads of types A and B for different values of power-law index, slenderness and skin-core-skin thickness ratio. The results are compared with those obtained from zero normal strain models, which are based on third-order beam theory (TBT) [27], higher-order beam theory (HOBT) [28] and from non-zero normal strain model, which is based on TBT [22]. It can be observed from these tables that the present results agree very well with the previous solutions for both zero normal strain and non-zero normal strain cases. It is worthy of note that the inclusion of the normal strain results in an increase in the natural frequencies and critical buckling loads. The results obtained by three higher-order shear deformation theories considered in this study (SBT, HBT and EBT) are indeed very similar to each other. Moreover, the maximum values were always obtained with EBT. As expected, for type A, when $k = 0$ (fully ceramic beam, see Eq. (2)), fundamental natural frequencies and critical buckling loads are the same irrespective of the beam configuration. However, for type B, when $k = 0$, which corresponds to sandwich beam (see Eq. (3)), the results change with change in the beam configuration. The maximum values are obtained with (1-8-1) and the minimum values with (2-1-1) configuration. As k increases, these orders are changing and the minimum values are obtained from the (1-8-1) configuration at large k values. For all configurations, it can be seen that the natural frequencies and critical buckling loads decrease in a rapid manner with an increase in k. For type A, the decrease is much more significant in the (2-1-2) configuration and least significant in the (1-8-1) configuration (Figs. 2a and 3a). However, for type B, the variation is generally less pronounced and the maximum variation is recorded in the (1-8-1) configuration (Figs. 2b and 3b). For all cases, the highest fundamental frequency and critical buckling load value is obtained when $k = 0$, i.e the beam is fully ceramic for type A or the beam has the highest portion of ceramic phase compared with others for type B. This behaviour is somewhat expected since an increase in the power-law index value results in decrease in the elastic modulus. The beam therefore becomes more flexible; buckles at much lower load, and the fundamental frequency decreases. Figs. 3 and 4 show the effect of shear deformation on the fundamental frequencies and critical buckling loads for varying L/h values. It can be seen that increase in L/h results in an increase in the fundamental frequencies and critical buckling loads for both types. However, it should be noted

that although similar behaviour were obtained for both types A and B, the variation of frequency and critical buckling load values between different beam configurations is more pronounced in type A than type B.

Finally, the first three natural fundamental frequencies of (1-8-1) sandwich beams of types A and B are presented in Tables 9 and 10 while Fig. 6 shows the corresponding mode shapes. It can be seen again that all shear deformation beam theories give the same frequencies. For symmetric configuration (1-8-1, type A), all vibration mode shapes show triply coupled mode (axial-shear-flexural), however, for unsymmetric one (1-8-1, type B), fourfold coupled modes (axial-shear-flexural-stretching) are observed. These fourfold modes highlight the effect of normal strain on the vibration and buckling of sandwich beams.

6. Conclusions

Various quasi-3D theories for vibration and buckling of FG sandwich beams of two types, FG skins-homogeneous core (type A) and homogeneous skins-FG core (type B), are developed. The equations of motion are derived from Hamilton's principle and analytical solution for simply supported beams is presented. The effects of power-law index, slenderness and skin-core-skin thickness ratio on the critical buckling loads and natural frequencies of FG sandwich beams are investigated. The following points can be outlined from the present study:

1. The results obtained by three higher-order shear deformation theories considered in this study (SBT, HBT and EBT) are indeed very similar to each other, and agree well with the existing solutions.
2. The highest fundamental natural frequencies and critical buckling loads is obtained when power-law index $k = 0$, i.e the beam is fully ceramic for type A or the beam has the highest portion of ceramic phase compared with others for type B.
3. The increase of the power-law index leads to a decrease in the natural frequencies and critical buckling loads for both types.
4. The inclusion of the normal strain results in an increase in the natural frequencies and critical buckling loads for both types.

7. Acknowledgements

The authors would like to thank Dr. Huu-Tai Thai at The University of New South Wales for discussion about quasi-3D theories and Matlab codes. The authors gratefully acknowledge the financial support from Newton Research Collaboration Programme of Royal Academy of Engineering

(NRCP/1415/185) and Basic Research Laboratory Program of the National Research Foundation of Korea (NRF) funded by the Ministry of Education, Science and Technology (2010-0019373 and 2012R1A2A1A01007405)

References

[1] T.-K. Nguyen, T. P. Vo, H.-T. Thai. Vibration and buckling analysis of functionally graded sandwich plates with improved transverse shear stiffness based on the first-order shear deformation theory, Proceedings of the Institution of Mechanical Engineers, Part C: Journal of Mechanical Engineering Science 228 (12) (2014) 2110 – 2131.

[2] H.-T. Thai, T.-K. Nguyen, T. P. Vo, J. Lee, Analysis of functionally graded sandwich plates using a new first-order shear deformation theory, European Journal of Mechanics - A/Solids 45 (2014) 211 – 225.

[3] A. M. Zenkour, A comprehensive analysis of functionally graded sandwich plates: Part 1-deflection and stresses, International Journal of Solids and Structures 42 (18-19) (2005) 5224 – 5242.

[4] A. M. Zenkour, A comprehensive analysis of functionally graded sandwich plates: Part 2-buckling and free vibration, International Journal of Solids and Structures 42 (18-19) (2005) 5243 – 5258.

[5] S. Merdaci, A. Tounsi, M. Houari, I. Mechab, H. Hebali, S. Benyoucef, Two new refined shear displacement models for functionally graded sandwich plates, Archive of Applied Mechanics 81 (2011) 1507–1522.

[6] N. E. Meiche, A. Tounsi, N. Ziane, I. Mechab, E. A. Adda.Bedia, A new hyperbolic shear deformation theory for buckling and vibration of functionally graded sandwich plate, International Journal of Mechanical Sciences 53 (4) (2011) 237 – 247.

[7] S. Natarajan, G. Manickam, Bending and vibration of functionally graded material sandwich plates using an accurate theory, Finite Elements in Analysis and Design 57 (2012) 32 – 42.

[8] A. Hamidi, M. Zidi, M. S. A. Houari, A. Tounsi, A new four variable refined plate theory for bending response of functionally graded sandwich plates under thermomechanical loading, Composites Part B: Engineering (0) (2012) In Press.

[9] M. Sobhy, Buckling and free vibration of exponentially graded sandwich plates resting on elastic foundations under various boundary conditions, Composite Structures 99 (2013) 76 – 87.

[10] V.-H. Nguyen, T.-K. Nguyen, H.-T. Thai, T. P. Vo, A new inverse trigonometric shear deformation theory for isotropic and functionally graded sandwich plates, Composites Part B: Engineering 66 (0) (2014) 233–246.

[11] C. H. Thai, S. Kulasegaram, L. V. Tran, H. Nguyen-Xuan, Generalized shear deformation theory for functionally graded isotropic and sandwich plates based on isogeometric approach, Computers & Structures 141 (0) (2014) 94 – 112.

[12] E. Carrera, S. Brischetto, M. Cinefra, M. Soave, Effects of thickness stretching in functionally graded plates and shells, Composites Part B: Engineering 42 (2) (2011) 123 – 133.

[13] S. Brischetto, Classical and mixed advanced models for sandwich plates embedding functionally graded cores, Journal of Mechanics of Materials and Structures 4 (2009) 13–33.

[14] A. M. A. Neves, A. J. M. Ferreira, E. Carrera, M. Cinefra, R. M. N. Jorge, C. M. M. Soares, Buckling analysis of sandwich plates with functionally graded skins using a new quasi-3D hyperbolic sine shear deformation theory and collocation with radial basis functions, Journal of Applied Mathematics and Mechanics 92 (2012) 749–766.

[15] A. M. A. Neves, A. J. M. Ferreira, E. Carrera, M. Cinefra, C. M. C. Roque, R. M. N. Jorge, C. M. M. Soares, Static, free vibration and buckling analysis of isotropic and sandwich functionally graded plates using a quasi-3D higher-order shear deformation theory and a meshless technique, Composites Part B: Engineering 44 (2013) 657–674.

[16] A. M. Zenkour, Bending analysis of functionally graded sandwich plates using a simple four-unknown shear and normal deformations theory, Journal of Sandwich Structures and Materials 15 (2013) 629–656.

[17] A. M. Zenkour, Bending analysis of functionally graded sandwich plates using a simple four-unknown shear and normal deformations theory, Journal of Sandwich Structures and Materials 15 (6) (2013) 629–656.

[18] A. Bessaim, M. S. Houari, A. Tounsi, S. Mahmoud, E. A. Adda Bedia, A new higher-order shear and normal deformation theory for the static and free vibration analysis of sandwich plates with functionally graded isotropic face sheets, Journal of Sandwich Structures and Materials 15 (2013) 671–703.

[19] Z. Belabed, M. S. A. Houari, A. Tounsi, S. R. Mahmoud, O. A. Beg, An efficient and simple higher order shear and normal deformation theory for functionally graded material (FGM) plates, Composites Part B: Engineering 60 (0) (2014) 274 – 283.

[20] E. Carrera, G. Giunta, M. Petrolo, Beam structures: classical and advanced theories, John Wiley & Sons, 2011.

[21] D. S. Mashat, E. Carrera, A. M. Zenkour, S. A. A. Khateeb, M. Filippi, Free vibration of FGM layered beams by various theories and finite elements, Composites Part B: Engineering 59 (0) (2014) 269 – 278.

[22] T. P. Vo, H.-T. Thai, T.-K. Nguyen, Inam, F., J. Lee, A quasi-3D theory for vibration and buckling of functionally graded sandwich beams, Composite Structures 119 (2015) 1 – 12.

[23] J. N. Reddy, Mechanics of laminated composite plates and shells: theory and analysis, CRC, 2004.

[24] M. Touratier, An efficient standard plate theory, International Journal of Engineering Science 29 (8) (1991) 901 – 916.

[25] K. P. Soldatos, A transverse shear deformation theory for homogeneous monoclinic plates, Acta mechanica 94 (3) (1992) 195–220.

[26] Karama, M.; Afaq, K. S., Mistou, S., Mechanical behaviour of laminated composite beam by the new multi-layered laminated composite structures model with transverse shear stress continuity, International Journal of Solids and Structures 40 (2003) 1525–1546.

[27] T. P. Vo, H.-T. Thai, T.-K. Nguyen, A. Maheri, J. Lee, Finite element model for vibration and buckling of functionally graded sandwich beams based on a refined shear deformation theory, Engineering Structures 64 (0) (2014) 12 – 22.

[28] T.-K. Nguyen, B.-D. Nguyen, A new higher-order shear deformation theory for static, buckling and free vibration analysis of functionally graded sandwich beams, Journal of Sandwich Structures and Materials 2015, To appear.

CAPTIONS OF TABLES

Table 1: The fundamental natural frequencies $\bar{\omega}$ of FG sandwich beams (Type A, L/h=5)

Table 2: The fundamental natural frequencies $\bar{\omega}$ of FG sandwich beams (Type A, L/h=20)

Table 3: The fundamental natural frequencies $\bar{\omega}$ of FG sandwich beams (Type B, L/h=5)

Table 4: The fundamental natural frequencies $\bar{\omega}$ of FG sandwich beams (Type B, L/h=20)

Table 5: The critical buckling loads $\bar{P}_{cr}$ of FG sandwich beams (Type A, L/h=5).

Table 6: The critical buckling loads $\bar{P}_{cr}$ of FG sandwich beams (Type A, L/h=20).

Table 7: The critical buckling loads $\bar{P}_{cr}$ of FG sandwich beams (Type B, L/h=5).

Table 8: The critical buckling loads $\bar{P}_{cr}$ of FG sandwich beams (Type B, L/h=20).

Table 9: The first three natural frequencies of (1-8-1) FG sandwich beams of Type A.

Table 10: The first three natural frequencies of (1-8-1) FG sandwich beams of Type B.

Table 1: The fundamental natural frequencies $\bar{\omega}$ of FG sandwich beams (Type A, L/h=5).

k	Theory	2-1-2	2-1-1	1-1-1	2-2-1	1-2-1	1-8-1
0	TBT [27] ($\varepsilon_z = 0$)	5.1528	5.1528	5.1528	5.1528	5.1528	5.1528
	HOBT [28] ($\varepsilon_z = 0$)	5.1528	5.1528	5.1528	5.1528	5.1528	-
	SBT ($\varepsilon_z = 0$)	5.1531	5.1531	5.1531	5.1531	5.1531	5.1531
	HBT ($\varepsilon_z = 0$)	5.1527	5.1527	5.1527	5.1527	5.1527	5.1527
	EBT ($\varepsilon_z = 0$)	5.1542	5.1542	5.1542	5.1542	5.1542	5.1542
	Quasi-3D [22] (TBT, $\varepsilon_z \neq 0$)	5.1618	5.1618	5.1618	5.1618	5.1618	5.1618
	Quasi-3D (SBT, $\varepsilon_z \neq 0$)	5.1665	5.1665	5.1665	5.1665	5.1665	5.1665
	Quasi-3D (HBT, $\varepsilon_z \neq 0$)	5.1615	5.1615	5.1615	5.1615	5.1615	5.1615
	Quasi-3D (EBT, $\varepsilon_z \neq 0$)	5.1789	5.1789	5.1789	5.1789	5.1789	5.1789
1	TBT [27] ($\varepsilon_z = 0$)	3.7298	3.8187	3.8755	3.9896	4.1105	4.6795
	HOBT [28] ($\varepsilon_z = 0$)	3.7298	3.8206	3.8756	3.9911	4.1105	-
	SBT ($\varepsilon_z = 0$)	3.7303	3.8209	3.8759	3.9913	4.1104	4.6790
	HBT ($\varepsilon_z = 0$)	3.7297	3.8206	3.8755	3.9911	4.1106	4.6796
	EBT ($\varepsilon_z = 0$)	3.7311	3.8215	3.8764	3.9917	4.1105	4.6790
	Quasi-3D [22] (TBT, $\varepsilon_z \neq 0$)	3.7369	3.8301	3.8830	4.0005	4.1185	4.6884
	Quasi-3D (SBT, $\varepsilon_z \neq 0$)	3.7400	3.8349	3.8859	4.0046	4.1210	4.6909
	Quasi-3D (HBT, $\varepsilon_z \neq 0$)	3.7366	3.8314	3.8827	4.0016	4.1183	4.6882
	Quasi-3D (EBT, $\varepsilon_z \neq 0$)	3.7478	3.8425	3.8935	4.0120	4.1282	4.6989
5	TBT [27] ($\varepsilon_z = 0$)	2.8439	2.9746	3.0181	3.1928	3.3771	4.3501
	HOBT [28] ($\varepsilon_z = 0$)	2.8440	2.9789	3.0181	3.1965	3.3771	-
	SBT ($\varepsilon_z = 0$)	2.8451	2.9796	3.0188	3.1970	3.3772	4.3492
	HBT ($\varepsilon_z = 0$)	2.8438	2.9788	3.0180	3.1964	3.3771	4.3502
	EBT ($\varepsilon_z = 0$)	2.8463	2.9804	3.0197	3.1976	3.3773	4.3487
	Quasi-3D [22] (TBT, $\varepsilon_z \neq 0$)	2.8489	2.9912	3.0238	3.2087	3.3840	4.3589
	Quasi-3D (SBT, $\varepsilon_z \neq 0$)	2.8526	3.0002	3.0271	3.2158	3.3864	4.3603
	Quasi-3D (HBT, $\varepsilon_z \neq 0$)	2.8486	2.9944	3.0236	3.2115	3.3838	4.3588
	Quasi-3D (EBT, $\varepsilon_z \neq 0$)	2.8609	3.0091	3.0349	3.2231	3.3926	4.3659
10	TBT [27] ($\varepsilon_z = 0$)	2.7355	2.8669	2.8808	3.0588	3.2356	4.2776
	HOBT [28] ($\varepsilon_z = 0$)	2.7356	2.8715	2.8809	3.0629	3.2357	-
	SBT ($\varepsilon_z = 0$)	2.7369	2.8723	2.8817	3.0635	3.2359	4.2767
	HBT ($\varepsilon_z = 0$)	2.7353	2.8714	2.8807	3.0628	3.2356	4.2777
	EBT ($\varepsilon_z = 0$)	2.7384	2.8732	2.8828	3.0642	3.2362	4.2762
	Quasi-3D [22] (TBT, $\varepsilon_z \neq 0$)	2.7400	2.8839	2.8860	3.0757	3.2422	4.2864
	Quasi-3D (SBT, $\varepsilon_z \neq 0$)	2.7438	2.8939	2.8896	3.0839	3.2449	4.2876
	Quasi-3D (HBT, $\varepsilon_z \neq 0$)	2.7397	2.8872	2.8858	3.0788	3.2420	4.2863
	Quasi-3D (EBT, $\varepsilon_z \neq 0$)	2.7524	2.9037	2.8979	3.0919	3.2515	4.2929

Table 2: The fundamental natural frequencies $\bar{\omega}$ of FG sandwich beams (Type A, L/h=20).

k	Theory	2-1-2	2-1-1	1-1-1	2-2-1	1-2-1	1-8-1
0	TBT [27] ($\varepsilon_z = 0$)	5.4603	5.4603	5.4603	5.4603	5.4603	5.4603
	HOBT [28] ($\varepsilon_z = 0$)	5.4603	5.4603	5.4603	5.4603	5.4603	-
	SBT ($\varepsilon_z = 0$)	5.4603	5.4603	5.4603	5.4603	5.4603	5.4603
	HBT ($\varepsilon_z = 0$)	5.4603	5.4603	5.4603	5.4603	5.4603	5.4603
	EBT ($\varepsilon_z = 0$)	5.4604	5.4604	5.4604	5.4604	5.4604	5.4604
	Quasi-3D [22] (TBT, $\varepsilon_z \neq 0$)	5.4610	5.4610	5.4610	5.4610	5.4610	5.4610
	Quasi-3D (SBT, $\varepsilon_z \neq 0$)	5.4650	5.4650	5.4650	5.4650	5.4650	5.4650
	Quasi-3D (HBT, $\varepsilon_z \neq 0$)	5.4610	5.4610	5.4610	5.4610	5.4610	5.4610
	Quasi-3D (EBT, $\varepsilon_z \neq 0$)	5.4771	5.4771	5.4771	5.4771	5.4771	5.4771
1	TBT [27] ($\varepsilon_z = 0$)	3.8768	3.9774	4.0328	4.1602	4.2889	4.9233
	HOBT [28] ($\varepsilon_z = 0$)	3.8768	3.9775	4.0328	4.1603	4.2889	-
	SBT ($\varepsilon_z = 0$)	3.8768	3.9776	4.0328	4.1603	4.2889	4.9233
	HBT ($\varepsilon_z = 0$)	3.8768	3.9775	4.0328	4.1603	4.2889	4.9233
	EBT ($\varepsilon_z = 0$)	3.8769	3.9776	4.0329	4.1603	4.2889	4.9233
	Quasi-3D [22] (TBT, $\varepsilon_z \neq 0$)	3.8773	3.9822	4.0333	4.1641	4.2895	4.9239
	Quasi-3D (SBT, $\varepsilon_z \neq 0$)	3.8800	3.9852	4.0360	4.1668	4.2921	4.9268
	Quasi-3D (HBT, $\varepsilon_z \neq 0$)	3.8773	3.9822	4.0333	4.1641	4.2895	4.9240
	Quasi-3D (EBT, $\varepsilon_z \neq 0$)	3.8875	3.9928	4.0435	4.1743	4.2997	4.9353
5	TBT [27] ($\varepsilon_z = 0$)	2.9310	3.0773	3.1111	3.3028	3.4921	4.5554
	HOBT [28] ($\varepsilon_z = 0$)	2.9311	3.0776	3.1111	3.3030	3.4921	-
	SBT ($\varepsilon_z = 0$)	2.9311	3.0776	3.1111	3.3031	3.4921	4.5553
	HBT ($\varepsilon_z = 0$)	2.9310	3.0775	3.1111	3.3030	3.4921	4.5554
	EBT ($\varepsilon_z = 0$)	2.9312	3.0777	3.1112	3.3031	3.4921	4.5553
	Quasi-3D [22] (TBT, $\varepsilon_z \neq 0$)	2.9314	3.0891	3.1115	3.3133	3.4926	4.5560
	Quasi-3D (SBT, $\varepsilon_z \neq 0$)	2.9341	3.0943	3.1142	3.3171	3.4951	4.5582
	Quasi-3D (HBT, $\varepsilon_z \neq 0$)	2.9314	3.0890	3.1115	3.3133	3.4926	4.5560
	Quasi-3D (EBT, $\varepsilon_z \neq 0$)	2.9416	3.1030	3.1216	3.3244	3.5016	4.5647
10	TBT [27] ($\varepsilon_z = 0$)	2.8188	2.9662	2.9662	3.1613	3.3406	4.4749
	HOBT [28] ($\varepsilon_z = 0$)	2.8188	2.9665	2.9662	3.1616	3.3406	-
	SBT ($\varepsilon_z = 0$)	2.8189	2.9665	2.9662	3.1616	3.3406	4.4749
	HBT ($\varepsilon_z = 0$)	2.8188	2.9665	2.9662	3.1615	3.3406	4.4749
	EBT ($\varepsilon_z = 0$)	2.8190	2.9666	2.9663	3.1616	3.3407	4.4748
	Quasi-3D [22] (TBT, $\varepsilon_z \neq 0$)	2.8191	2.9786	2.9665	3.1732	3.3411	4.4755
	Quasi-3D (SBT, $\varepsilon_z \neq 0$)	2.8217	2.9846	2.9694	3.1777	3.3437	4.4777
	Quasi-3D (HBT, $\varepsilon_z \neq 0$)	2.8191	2.9785	2.9665	3.1732	3.3411	4.4756
	Quasi-3D (EBT, $\varepsilon_z \neq 0$)	2.8292	2.9941	2.9771	3.1856	3.3505	4.4839

Table 3: The fundamental natural frequencies $\bar{\omega}$ of FG sandwich beams (Type B, L/h=5).

k	Theory	2-1-2	2-1-1	1-1-1	2-2-1	1-2-1	1-8-1
0	TBT [27] ($\varepsilon_z = 0$)	-	-	-	-	-	4.6694
	SBT ($\varepsilon_z = 0$)	3.6637	3.5227	3.8162	3.6637	4.0698	4.6719
	HBT ($\varepsilon_z = 0$)	3.6620	3.5218	3.8146	3.6620	4.0689	4.6722
	EBT ($\varepsilon_z = 0$)	3.6655	3.5238	3.8179	3.6655	4.0709	4.6720
	Quasi-3D [22] (TBT, $\varepsilon_z \neq 0$)	-	-	-	-	-	4.6829
	Quasi-3D (SBT, $\varepsilon_z \neq 0$)	3.7202	3.5894	3.8625	3.7202	4.1023	4.6872
	Quasi-3D (HBT, $\varepsilon_z \neq 0$)	3.7126	3.5810	3.8570	3.7126	4.0996	4.6850
	Quasi-3D (EBT, $\varepsilon_z \neq 0$)	3.7314	3.6009	3.8722	3.7314	4.1103	4.6953
1	TBT [27] ($\varepsilon_z = 0$)	-	-	-	-	-	3.8243
	SBT ($\varepsilon_z = 0$)	3.5466	3.4897	3.5878	3.5289	3.6640	3.8504
	HBT ($\varepsilon_z = 0$)	3.5458	3.4915	3.5871	3.5294	3.6635	3.8501
	EBT ($\varepsilon_z = 0$)	3.5476	3.4882	3.5888	3.5288	3.6649	3.8511
	Quasi-3D [22] (TBT, $\varepsilon_z \neq 0$)	-	-	-	-	-	3.8708
	Quasi-3D (SBT, $\varepsilon_z \neq 0$)	3.6119	3.5559	3.6506	3.5928	3.7220	3.8962
	Quasi-3D (HBT, $\varepsilon_z \neq 0$)	3.6039	3.5518	3.6434	3.5875	3.7162	3.8926
	Quasi-3D (EBT, $\varepsilon_z \neq 0$)	3.6229	3.5629	3.6609	3.6013	3.7313	3.9042
5	TBT [27] ($\varepsilon_z = 0$)	-	-	-	-	-	3.4474
	SBT ($\varepsilon_z = 0$)	3.4860	3.4780	3.4822	3.4819	3.4889	3.4843
	HBT ($\varepsilon_z = 0$)	3.4866	3.4834	3.4840	3.4873	3.4922	3.4873
	EBT ($\varepsilon_z = 0$)	3.4858	3.4724	3.4709	3.4733	3.4746	3.4504
	Quasi-3D [22] (TBT, $\varepsilon_z \neq 0$)	-	-	-	-	-	3.5011
	Quasi-3D (SBT, $\varepsilon_z \neq 0$)	3.5548	3.5393	3.5499	3.5398	3.5529	3.5351
	Quasi-3D (HBT, $\varepsilon_z \neq 0$)	3.5481	3.5409	3.5454	3.5420	3.5512	3.5353
	Quasi-3D (EBT, $\varepsilon_z \neq 0$)	3.5642	3.5407	3.5572	3.5410	3.5575	3.5386
10	TBT [27] ($\varepsilon_z = 0$)	-	-	-	-	-	3.4204
	SBT ($\varepsilon_z = 0$)	3.4782	3.4778	3.4734	3.4784	3.4791	3.4527
	HBT ($\varepsilon_z = 0$)	3.4792	3.4840	3.4763	3.4846	3.4843	3.4562
	EBT ($\varepsilon_z = 0$)	3.4775	3.4724	3.4709	3.4733	3.4746	3.4504
	Quasi-3D [22] (TBT, $\varepsilon_z \neq 0$)	-	-	-	-	-	3.4671
	Quasi-3D (SBT, $\varepsilon_z \neq 0$)	3.5471	3.5371	3.5407	3.5325	3.5407	3.4952
	Quasi-3D (HBT, $\varepsilon_z \neq 0$)	3.5412	3.5400	3.5378	3.5365	3.5420	3.4975
	Quasi-3D (EBT, $\varepsilon_z \neq 0$)	3.5559	3.5372	3.5463	3.5320	3.5425	3.4971

Table 4: The fundamental natural frequencies $\bar{\omega}$ of FG sandwich beams (Type B, L/h=20).

k	Theory	2-1-2	2-1-1	1-1-1	2-2-1	1-2-1	1-8-1
0	TBT [27] ($\varepsilon_z = 0$)	-	-	-	-	-	4.9141
	SBT ($\varepsilon_z = 0$)	3.8137	3.6806	3.9719	3.8137	4.2446	4.9142
	HBT ($\varepsilon_z = 0$)	3.8135	3.6805	3.9718	3.8135	4.2445	4.9142
	EBT ($\varepsilon_z = 0$)	3.8138	3.6806	3.9720	3.8138	4.2446	4.9142
	Quasi-3D [22] (TBT, $\varepsilon_z \neq 0$)	-	-	-	-	-	4.9196
	Quasi-3D (SBT, $\varepsilon_z \neq 0$)	3.8697	3.7486	4.0162	3.8697	4.2728	4.9218
	Quasi-3D (HBT, $\varepsilon_z \neq 0$)	3.8636	3.7405	4.0124	3.8636	4.2715	4.9198
	Quasi-3D (EBT, $\varepsilon_z \neq 0$)	3.8797	3.7598	4.0246	3.8797	4.2801	4.9302
1	TBT [27] ($\varepsilon_z = 0$)	-	-	-	-	-	4.0462
	SBT ($\varepsilon_z = 0$)	3.7073	3.6878	3.7534	3.7176	3.8388	4.0478
	HBT ($\varepsilon_z = 0$)	3.7072	3.6879	3.7534	3.7177	3.8387	4.0478
	EBT ($\varepsilon_z = 0$)	3.7073	3.6877	3.7535	3.7176	3.8388	4.0478
	Quasi-3D [22] (TBT, $\varepsilon_z \neq 0$)	-	-	-	-	-	4.0874
	Quasi-3D (SBT, $\varepsilon_z \neq 0$)	3.7736	3.7567	3.8168	3.7833	3.8967	4.0918
	Quasi-3D (HBT, $\varepsilon_z \neq 0$)	3.7661	3.7505	3.8102	3.7772	3.8914	4.0887
	Quasi-3D (EBT, $\varepsilon_z \neq 0$)	3.7844	3.7659	3.8270	3.7927	3.9058	4.0995
5	TBT [27] ($\varepsilon_z = 0$)	-	-	-	-	-	3.7363
	SBT ($\varepsilon_z = 0$)	3.6617	3.7226	3.6754	3.7377	3.7079	3.7388
	HBT ($\varepsilon_z = 0$)	3.6618	3.7230	3.6756	3.7382	3.7082	3.7391
	EBT ($\varepsilon_z = 0$)	3.6617	3.7222	3.6753	3.7373	3.7077	3.7387
	Quasi-3D [22] (TBT, $\varepsilon_z \neq 0$)	-	-	-	-	-	3.7871
	Quasi-3D (SBT, $\varepsilon_z \neq 0$)	3.7327	3.7876	3.7458	3.7990	3.7748	3.7917
	Quasi-3D (HBT, $\varepsilon_z \neq 0$)	3.7251	3.7840	3.7392	3.7963	3.7699	3.7894
	Quasi-3D (EBT, $\varepsilon_z \neq 0$)	3.7432	3.7941	3.7554	3.8049	3.7828	3.7976
10	TBT [27] ($\varepsilon_z = 0$)	-	-	-	-	-	3.7387
	SBT ($\varepsilon_z = 0$)	3.6591	3.7351	3.6784	3.7548	3.7210	3.7410
	HBT ($\varepsilon_z = 0$)	3.6591	3.7356	3.6786	3.7553	3.7214	3.7413
	EBT ($\varepsilon_z = 0$)	3.6590	3.7346	3.6782	3.7544	3.7206	3.7408
	Quasi-3D [22] (TBT, $\varepsilon_z \neq 0$)	-	-	-	-	-	3.7825
	Quasi-3D (SBT, $\varepsilon_z \neq 0$)	3.7304	3.7982	3.7487	3.8125	3.7862	3.7851
	Quasi-3D (HBT, $\varepsilon_z \neq 0$)	3.7231	3.7954	3.7427	3.8109	3.7825	3.7848
	Quasi-3D (EBT, $\varepsilon_z \neq 0$)	3.7408	3.8039	3.7576	3.8171	3.7928	3.7892

Table 5: The critical buckling loads $\bar{P}_{cr}$ of FG sandwich beams (Type A, L/h=5).

k	Theory	2-1-2	2-1-1	1-1-1	2-2-1	1-2-1	1-8-1
0	TBT [27] ($\varepsilon_z = 0$)	48.5959	48.5959	48.5959	48.5959	48.5959	48.5959
	HOT [28] ($\varepsilon_z = 0$)	48.5960	48.5960	48.5960	48.5960	48.5960	-
	SBT ($\varepsilon_z = 0$)	48.6037	48.6037	48.6037	48.6037	48.6037	48.6037
	HBT ($\varepsilon_z = 0$)	48.5960	48.5960	48.5960	48.5960	48.5960	48.5960
	EBT ($\varepsilon_z = 0$)	48.6253	48.6253	48.6253	48.6253	48.6253	48.6253
	Quasi-3D [22] (TBT, $\varepsilon_z \neq 0$)	49.5906	49.5906	49.5906	49.5906	49.5906	49.5906
	Quasi-3D (SBT, $\varepsilon_z \neq 0$)	49.6710	49.6710	49.6710	49.6710	49.6710	49.6710
	Quasi-3D (HBT, $\varepsilon_z \neq 0$)	49.5890	49.5890	49.5890	49.5890	49.5890	49.5890
	Quasi-3D (EBT, $\varepsilon_z \neq 0$)	49.8730	49.8730	49.8730	49.8730	49.8730	49.8730
1	TBT [27] ($\varepsilon_z = 0$)	22.2108	23.5246	24.5596	26.3611	28.4447	38.7838
	HOT [28] ($\varepsilon_z = 0$)	22.2113	23.5246	24.5598	26.3609	28.4444	-
	SBT ($\varepsilon_z = 0$)	22.2185	23.5289	24.5641	26.3634	28.4429	38.7751
	HBT ($\varepsilon_z = 0$)	22.2100	23.5240	24.5590	26.3610	28.4450	38.7850
	EBT ($\varepsilon_z = 0$)	22.2289	23.5366	24.5715	26.3696	28.4450	38.7753
	Quasi-3D [22] (TBT, $\varepsilon_z \neq 0$)	22.7065	24.0838	25.1075	26.9764	29.0755	39.6144
	Quasi-3D (SBT, $\varepsilon_z \neq 0$)	22.7240	24.1010	25.1200	26.9890	29.0820	39.6290
	Quasi-3D (HBT, $\varepsilon_z \neq 0$)	22.7070	24.0840	25.1090	26.9780	29.0780	39.6170
	Quasi-3D (EBT, $\varepsilon_z \neq 0$)	22.7870	24.1650	25.1830	27.0540	29.1440	39.7230
5	TBT [27] ($\varepsilon_z = 0$)	11.6676	13.0270	13.7212	15.7307	18.0914	32.7725
	HOT [28] ($\varepsilon_z = 0$)	11.6685	13.0272	13.7218	15.7307	18.0914	-
	SBT ($\varepsilon_z = 0$)	11.6778	13.0332	13.7286	15.7356	18.0927	32.7589
	HBT ($\varepsilon_z = 0$)	11.6670	13.0260	13.7210	15.7300	18.0910	32.7740
	EBT ($\varepsilon_z = 0$)	11.6888	11.8518	12.2782	14.2126	16.3846	31.5042
	Quasi-3D [22] (TBT, $\varepsilon_z \neq 0$)	11.9301	13.3924	14.0353	16.1605	18.5092	33.4958
	Quasi-3D (SBT, $\varepsilon_z \neq 0$)	11.9520	13.4250	14.0500	16.1800	18.5090	33.4820
	Quasi-3D (HBT, $\varepsilon_z \neq 0$)	11.9300	13.3900	14.0360	16.1600	18.5110	33.5000
	Quasi-3D (EBT, $\varepsilon_z \neq 0$)	12.0050	13.4830	14.0980	16.2280	18.5440	33.5260
10	TBT [27] ($\varepsilon_z = 0$)	10.5348	11.8370	12.2605	14.1995	16.3783	31.5265
	HOT [28] ($\varepsilon_z = 0$)	10.5356	11.8372	12.2611	14.1995	16.3787	-
	SBT ($\varepsilon_z = 0$)	10.5464	11.8437	12.2691	14.2053	16.3811	31.5127
	HBT ($\varepsilon_z = 0$)	10.5340	11.8360	12.2600	14.1980	16.3780	31.5280
	EBT ($\varepsilon_z = 0$)	10.5588	11.8518	12.2782	14.2126	16.3846	31.5042
	Quasi-3D [22] (TBT, $\varepsilon_z \neq 0$)	10.7689	12.1737	12.5393	14.5994	16.7574	32.2264
	Quasi-3D (SBT, $\varepsilon_z \neq 0$)	10.7940	12.2120	12.5580	14.6260	16.7610	32.2090
	Quasi-3D (HBT, $\varepsilon_z \neq 0$)	10.7680	12.1710	12.5390	14.5980	16.7590	32.2310
	Quasi-3D (EBT, $\varepsilon_z \neq 0$)	10.8482	12.2747	12.6096	14.6788	16.7987	32.2462

Table 6: The critical buckling loads $\bar{P}_{cr}$ of FG sandwich beams (Type A, L/h=20).

k	Theory	2-1-2	2-1-1	1-1-1	2-2-1	1-2-1	1-8-1
0	TBT [27] ($\varepsilon_z = 0$)	53.2364	53.2364	53.2364	53.2364	53.2364	53.2364
	HOT [28] ($\varepsilon_z = 0$)	53.2364	53.2364	53.2364	53.2364	53.2364	-
	SBT ($\varepsilon_z = 0$)	53.2369	53.2369	53.2369	53.2369	53.2369	53.2369
	HBT ($\varepsilon_z = 0$)	53.2360	53.2360	53.2360	53.2360	53.2360	53.2360
	EBT ($\varepsilon_z = 0$)	53.2384	53.2384	53.2384	53.2384	53.2384	53.2384
	Quasi-3D [22] (TBT, $\varepsilon_z \neq 0$)	53.3145	53.3145	53.3145	53.3145	53.3145	53.3145
	Quasi-3D (SBT, $\varepsilon_z \neq 0$)	53.3920	53.3920	53.3920	53.3920	53.3920	53.3920
	Quasi-3D (HBT, $\varepsilon_z \neq 0$)	53.3150	53.3150	53.3150	53.3150	53.3150	53.3150
	Quasi-3D (EBT, $\varepsilon_z \neq 0$)	53.6250	53.6250	53.6250	53.6250	53.6250	53.6250
1	TBT [27] ($\varepsilon_z = 0$)	23.4211	24.8796	25.9588	27.9540	30.2307	41.9004
	HOT [28] ($\varepsilon_z = 0$)	23.4212	24.8793	25.9588	27.9537	30.2307	-
	SBT ($\varepsilon_z = 0$)	23.4216	24.8796	25.9591	27.9539	30.2305	41.8997
	HBT ($\varepsilon_z = 0$)	23.4210	24.8790	25.9590	27.9540	30.2310	41.9010
	EBT ($\varepsilon_z = 0$)	23.4224	24.8801	25.9596	27.9543	30.2307	41.8997
	Quasi-3D [22] (TBT, $\varepsilon_z \neq 0$)	23.4572	24.9697	25.9989	28.0412	30.2774	41.9639
	Quasi-3D (SBT, $\varepsilon_z \neq 0$)	23.4880	25.0050	26.0320	28.0750	30.3130	42.0100
	Quasi-3D (HBT, $\varepsilon_z \neq 0$)	23.4580	24.9690	25.9990	28.0410	30.2780	41.9640
	Quasi-3D (EBT, $\varepsilon_z \neq 0$)	23.5760	25.0980	26.1260	28.1730	30.4160	42.1520
5	TBT [27] ($\varepsilon_z = 0$)	12.0883	13.5523	14.2284	16.3834	18.8874	35.0856
	HOT [28] ($\varepsilon_z = 0$)	12.0885	13.5519	14.2285	16.3829	18.8874	-
	SBT ($\varepsilon_z = 0$)	12.0890	13.5522	14.2289	16.3832	18.8875	35.0846
	HBT ($\varepsilon_z = 0$)	12.0880	13.5520	14.2280	16.3830	18.8870	35.0860
	EBT ($\varepsilon_z = 0$)	12.0897	13.5527	14.2294	16.3836	18.8876	35.0841
	Quasi-3D [22] (TBT, $\varepsilon_z \neq 0$)	12.1068	13.6717	14.2505	16.5069	18.9172	35.1400
	Quasi-3D (SBT, $\varepsilon_z \neq 0$)	12.1280	13.7150	14.2750	16.5420	18.9420	35.1710
	Quasi-3D (HBT, $\varepsilon_z \neq 0$)	12.1070	13.6690	14.2510	16.5050	18.9180	35.1410
	Quasi-3D (EBT, $\varepsilon_z \neq 0$)	12.1890	13.7900	14.3410	16.6120	19.0100	35.2680
10	TBT [27] ($\varepsilon_z = 0$)	10.9075	12.3084	12.6819	14.7525	17.0443	33.6843
	HOT [28] ($\varepsilon_z = 0$)	10.9074	12.3080	12.6819	14.7520	17.0445	-
	SBT ($\varepsilon_z = 0$)	10.9083	12.3084	12.6825	14.7523	17.0445	33.6833
	HBT ($\varepsilon_z = 0$)	10.9074	12.3078	12.6818	14.7518	17.0443	33.6845
	EBT ($\varepsilon_z = 0$)	10.9091	12.3089	12.6831	14.7528	17.0447	33.6827
	Quasi-3D [22] (TBT, $\varepsilon_z \neq 0$)	10.9239	12.4256	12.7014	14.8807	17.0712	33.7367
	Quasi-3D (SBT, $\varepsilon_z \neq 0$)	10.9430	12.4720	12.7250	14.9200	17.0960	33.7660
	Quasi-3D (HBT, $\varepsilon_z \neq 0$)	10.9240	12.4230	12.7020	14.8780	17.0720	33.7370
	Quasi-3D (EBT, $\varepsilon_z \neq 0$)	11.0004	12.5508	12.7898	14.9920	17.1635	33.8561

Table 7: The critical buckling loads $\bar{P}_{cr}$ of FG sandwich beams (Type B, L/h=5).

k	Theory	2-1-2	2-1-1	1-1-1	2-2-1	1-2-1	1-8-1
0	TBT [27] ($\varepsilon_z = 0$)	-	-	-	-	-	38.6762
	SBT ($\varepsilon_z = 0$)	21.5362	19.2300	23.8978	21.5362	27.9418	38.6706
	HBT ($\varepsilon_z = 0$)	21.5160	19.2200	23.8770	21.5160	27.9280	38.6770
	EBT ($\varepsilon_z = 0$)	21.5593	19.2428	23.9206	21.5593	27.9580	38.6735
	Quasi-3D [22] (TBT, $\varepsilon_z \neq 0$)	-	-	-	-	-	39.5558
	Quasi-3D (SBT, $\varepsilon_z \neq 0$)	22.4730	20.1690	24.8100	22.4730	28.8170	39.5700
	Quasi-3D (HBT, $\varepsilon_z \neq 0$)	22.3890	20.0840	24.7470	22.3890	28.7890	39.5580
	Quasi-3D (EBT, $\varepsilon_z \neq 0$)	22.5920	20.2820	24.9180	22.5920	28.9060	39.6700
1	TBT [27] ($\varepsilon_z = 0$)	-	-	-	-	-	22.9142
	SBT ($\varepsilon_z = 0$)	19.4881	18.0085	19.9376	18.5853	20.7812	22.9153
	HBT ($\varepsilon_z = 0$)	19.4790	18.0290	19.9300	18.5920	20.7750	22.9120
	EBT ($\varepsilon_z = 0$)	19.5004	17.9925	19.9490	18.5838	20.7913	22.9239
	Quasi-3D [22] (TBT, $\varepsilon_z \neq 0$)	-	-	-	-	-	23.7280
	Quasi-3D (SBT, $\varepsilon_z \neq 0$)	20.4220	18.8730	20.8620	19.4560	21.6860	23.7630
	Quasi-3D (HBT, $\varepsilon_z \neq 0$)	20.3420	18.8390	20.7890	19.4060	21.6260	23.7240
	Quasi-3D (EBT, $\varepsilon_z \neq 0$)	20.5320	18.9340	20.9660	19.5350	21.7800	23.8470
5	TBT [27] ($\varepsilon_z = 0$)	-	-	-	-	-	16.8604
	SBT ($\varepsilon_z = 0$)	18.3794	17.2978	18.0311	17.1527	17.7056	16.9228
	HBT ($\varepsilon_z = 0$)	18.3860	17.3560	18.0520	17.2090	17.7420	16.9550
	EBT ($\varepsilon_z = 0$)	18.3763	17.2468	18.0145	17.1052	17.6753	16.9007
	Quasi-3D [22] (TBT, $\varepsilon_z \neq 0$)	-	-	-	-	-	17.6062
	Quasi-3D (SBT, $\varepsilon_z \neq 0$)	19.2920	18.0770	18.9120	17.8950	18.5300	17.6010
	Quasi-3D (HBT, $\varepsilon_z \neq 0$)	19.2310	18.1020	18.8750	17.9230	18.5220	17.6060
	Quasi-3D (EBT, $\varepsilon_z \neq 0$)	19.3790	18.0790	18.9740	17.8970	18.5650	17.6310
10	TBT [27] ($\varepsilon_z = 0$)	-	-	-	-	-	16.2077
	SBT ($\varepsilon_z = 0$)	18.1939	17.1575	17.7665	16.8940	17.3365	16.1733
	HBT ($\varepsilon_z = 0$)	18.2060	17.2230	17.7990	16.9590	17.3920	16.2090
	EBT ($\varepsilon_z = 0$)	18.1856	17.1001	17.7383	16.8405	17.2879	16.1504
	Quasi-3D [22] (TBT, $\varepsilon_z \neq 0$)	-	-	-	-	-	16.7752
	Quasi-3D (SBT, $\varepsilon_z \neq 0$)	19.0980	17.9110	18.6280	17.5920	18.1200	16.7560
	Quasi-3D (HBT, $\varepsilon_z \neq 0$)	19.0450	17.9490	18.6080	17.6360	18.1410	16.7760
	Quasi-3D (EBT, $\varepsilon_z \neq 0$)	19.1769	17.9011	18.6721	17.5789	18.1258	16.7735

Table 8: The critical buckling loads $\bar{P}_{cr}$ of FG sandwich beams (Type B, L/h=20).

k	Theory	2-1-2	2-1-1	1-1-1	2-2-1	1-2-1	1-8-1
0	TBT [27] ($\varepsilon_z = 0$)	-	-	-	-	-	41.7477
	SBT ($\varepsilon_z = 0$)	22.6725	20.3528	25.1867	22.6725	29.6127	41.7468
	HBT ($\varepsilon_z = 0$)	22.6710	20.3520	25.1850	22.6710	29.6120	41.7470
	EBT ($\varepsilon_z = 0$)	22.6741	20.3537	25.1883	22.6741	29.6138	41.7469
	Quasi-3D [22] (TBT, $\varepsilon_z \neq 0$)	-	-	-	-	-	41.8917
	Quasi-3D (SBT, $\varepsilon_z \neq 0$)	23.3630	21.1270	25.7760	23.3630	30.0400	41.9250
	Quasi-3D (HBT, $\varepsilon_z \neq 0$)	23.2900	21.0370	25.7280	23.2900	30.0220	41.8940
	Quasi-3D (EBT, $\varepsilon_z \neq 0$)	23.4830	21.2530	25.8830	23.4830	30.1400	42.0650
1	TBT [27] ($\varepsilon_z = 0$)						24.6163
	SBT ($\varepsilon_z = 0$)	20.6491	19.4727	21.1659	19.9835	22.1389	24.6138
	HBT ($\varepsilon_z = 0$)	20.6480	19.4740	21.1650	19.9840	22.1390	24.6140
	EBT ($\varepsilon_z = 0$)	20.6499	19.4714	21.1667	19.9834	22.1396	24.6143
	Quasi-3D [22] (TBT, $\varepsilon_z \neq 0$)	-	-	-	-	-	25.1407
	Quasi-3D (SBT, $\varepsilon_z \neq 0$)	21.4110	20.2210	21.9040	20.7110	22.8310	25.1740
	Quasi-3D (HBT, $\varepsilon_z \neq 0$)	21.3260	20.1550	21.8280	20.6450	22.7690	25.1380
	Quasi-3D (EBT, $\varepsilon_z \neq 0$)	21.5320	20.3190	22.0200	20.8120	22.9370	25.2690
5	TBT [27] ($\varepsilon_z = 0$)	-	-	-	-	-	18.8976
	SBT ($\varepsilon_z = 0$)	19.6406	19.1891	19.4486	19.1470	19.3616	18.8925
	HBT ($\varepsilon_z = 0$)	19.6410	19.1940	19.4500	19.1510	19.3640	18.8950
	EBT ($\varepsilon_z = 0$)	19.6404	19.1851	19.4474	19.1432	19.3593	18.8907
	Quasi-3D [22] (TBT, $\varepsilon_z \neq 0$)	-	-	-	-	-	19.4285
	Quasi-3D (SBT, $\varepsilon_z \neq 0$)	20.4230	19.8780	20.2140	19.7950	20.0810	19.4460
	Quasi-3D (HBT, $\varepsilon_z \neq 0$)	20.3410	19.8410	20.1440	19.7660	20.0290	19.4220
	Quasi-3D (EBT, $\varepsilon_z \neq 0$)	20.5380	19.9460	20.3160	19.8550	20.1650	19.5060
10	TBT [27] ($\varepsilon_z = 0$)	-	-	-	-	-	18.4377
	SBT ($\varepsilon_z = 0$)	19.4974	19.1683	19.2869	19.0804	19.2022	18.4326
	HBT ($\varepsilon_z = 0$)	19.4980	19.1730	19.2890	19.0860	19.2060	18.4360
	EBT ($\varepsilon_z = 0$)	19.4968	19.1637	19.2848	19.0760	19.1984	18.4307
	Quasi-3D [22] (TBT, $\varepsilon_z \neq 0$)	-	-	-	-	-	18.8840
	Quasi-3D (SBT, $\varepsilon_z \neq 0$)	20.2790	19.8350	20.0450	19.6850	19.8940	18.8860
	Quasi-3D (HBT, $\varepsilon_z \neq 0$)	20.2000	19.8060	19.9810	19.6690	19.8560	18.8830
	Quasi-3D (EBT, $\varepsilon_z \neq 0$)	20.3909	19.8948	20.1393	19.7331	19.9639	18.9269

Table 9: The first three natural frequencies of (1-8-1) FG sandwich beams of Type A.

L/h	Mode	Theory	$k=0$	$k=1$	$k=2$	$k=5$	$k=10$
5	1	Quasi-3D (SBT, $\varepsilon_z \neq 0$)	5.1665	4.6909	4.5249	4.3603	4.2876
		Quasi-3D (HBT, $\varepsilon_z \neq 0$)	5.1615	4.6882	4.5229	4.3588	4.2863
		Quasi-3D (EBT, $\varepsilon_z \neq 0$)	5.1789	4.6989	4.5316	4.3659	4.2929
	2	Quasi-3D (SBT, $\varepsilon_z \neq 0$)	17.9979	16.5734	16.0648	15.5559	15.3301
		Quasi-3D (HBT, $\varepsilon_z \neq 0$)	17.9704	16.5638	16.0603	15.5554	15.3309
		Quasi-3D (EBT, $\varepsilon_z \neq 0$)	18.0493	16.6017	16.0861	15.5715	15.3437
	3	Quasi-3D (SBT, $\varepsilon_z \neq 0$)	34.5559	32.2016	31.3461	30.4860	30.1040
		Quasi-3D (HBT, $\varepsilon_z \neq 0$)	34.4802	32.1808	31.3417	30.4949	30.1171
		Quasi-3D (EBT, $\varepsilon_z \neq 0$)	34.6744	32.2585	31.3838	30.5077	30.1202
20	1	Quasi-3D (SBT, $\varepsilon_z \neq 0$)	5.4650	4.9268	4.7413	4.5582	4.4777
		Quasi-3D (HBT, $\varepsilon_z \neq 0$)	5.4610	4.9240	4.7388	4.5560	4.4756
		Quasi-3D (EBT, $\varepsilon_z \neq 0$)	5.4771	4.9353	4.7487	4.5647	4.4839
	2	Quasi-3D (SBT, $\varepsilon_z \neq 0$)	21.6003	19.5040	18.7795	18.0636	17.7483
		Quasi-3D (HBT, $\varepsilon_z \neq 0$)	21.5835	19.4928	18.7701	18.0555	17.7406
		Quasi-3D (EBT, $\varepsilon_z \neq 0$)	21.6488	19.5376	18.8085	18.0889	17.7723
	3	Quasi-3D (SBT, $\varepsilon_z \neq 0$)	47.6823	43.1601	41.5906	40.0369	39.3519
		Quasi-3D (HBT, $\varepsilon_z \neq 0$)	47.6413	43.1356	41.5708	40.0209	39.3369
		Quasi-3D (EBT, $\varepsilon_z \neq 0$)	47.7925	43.2342	41.6536	40.0911	39.4032

Table 10: The first three natural frequencies of (1-8-1) FG sandwich beams of Type B.

L/h	Mode	Theory	$k=0$	$k=1$	$k=2$	$k=5$	$k=10$
5	1	Quasi-3D (SBT, $\varepsilon_z \neq 0$)	4.6872	3.8962	3.6676	3.5351	3.4952
		Quasi-3D (HBT, $\varepsilon_z \neq 0$)	4.6850	3.8926	3.6639	3.5353	3.4975
		Quasi-3D (EBT, $\varepsilon_z \neq 0$)	4.6953	3.9042	3.6751	3.5386	3.4971
	2	Quasi-3D (SBT, $\varepsilon_z \neq 0$)	16.5703	13.7799	12.8270	12.0055	11.6626
		Quasi-3D (HBT, $\varepsilon_z \neq 0$)	16.5597	13.7604	12.8125	12.0189	11.6832
		Quasi-3D (EBT, $\varepsilon_z \neq 0$)	16.6007	13.8140	12.8550	12.0079	11.6608
	3	Quasi-3D (SBT, $\varepsilon_z \neq 0$)	32.2196	26.8401	24.7562	22.6123	21.6531
		Quasi-3D (HBT, $\varepsilon_z \neq 0$)	32.1917	26.7863	24.7201	22.6488	21.7014
		Quasi-3D (EBT, $\varepsilon_z \neq 0$)	32.2838	26.9209	24.8193	22.6105	21.6464
20	1	Quasi-3D (SBT, $\varepsilon_z \neq 0$)	4.9218	4.0918	3.8738	3.7917	3.7851
		Quasi-3D (HBT, $\varepsilon_z \neq 0$)	4.9198	4.0887	3.8698	3.7894	3.7848
		Quasi-3D (EBT, $\varepsilon_z \neq 0$)	4.9302	4.0995	3.8817	3.7976	3.7892
	2	Quasi-3D (SBT, $\varepsilon_z \neq 0$)	19.4851	16.1984	15.3158	14.9389	14.8801
		Quasi-3D (HBT, $\varepsilon_z \neq 0$)	19.4772	16.1858	15.3000	14.9323	14.8816
		Quasi-3D (EBT, $\varepsilon_z \neq 0$)	19.5185	16.2297	15.3470	14.9603	14.8941
	3	Quasi-3D (SBT, $\varepsilon_z \neq 0$)	43.1217	35.8463	33.8263	32.8188	32.5808
		Quasi-3D (HBT, $\varepsilon_z \neq 0$)	43.1032	35.8158	33.7916	32.8120	32.5925
		Quasi-3D (EBT, $\varepsilon_z \neq 0$)	43.1962	35.9173	33.8952	32.8594	32.6054

CAPTIONS OF FIGURES

Figure 1: Geometry and coordinate of a FG sandwich beam

Figure 2: Effect of power-law index k on fundamental frequency obtained from a quasi-3D (HBT, $\varepsilon_z \neq 0$).

Figure 3: Effect of power-law index k on critical buckling load obtained from a quasi-3D (HBT, $\varepsilon_z \neq 0$).

Figure 4: Effect of shear deformation on the fundamental frequency obtained from a quasi-3D (HBT, $\varepsilon_z \neq 0$).

Figure 5: Effect of shear deformation on the critical buckling loads obtained from a quasi-3D (HBT, $\varepsilon_z \neq 0$).

Figure 6**:** Vibration mode shapes of (1-8-1) sandwich beam (Types A and B, k=5, L/h=5) using a quasi-3D (HBT, $\varepsilon_z \neq 0$).

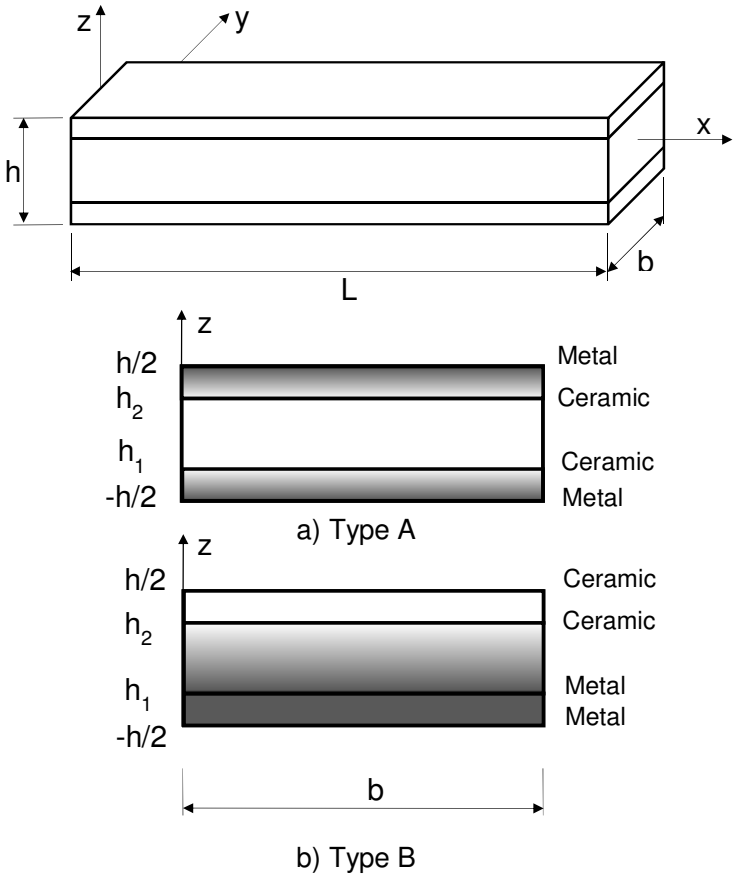

Figure 1: Geometry and coordinate of a FG sandwich beam.

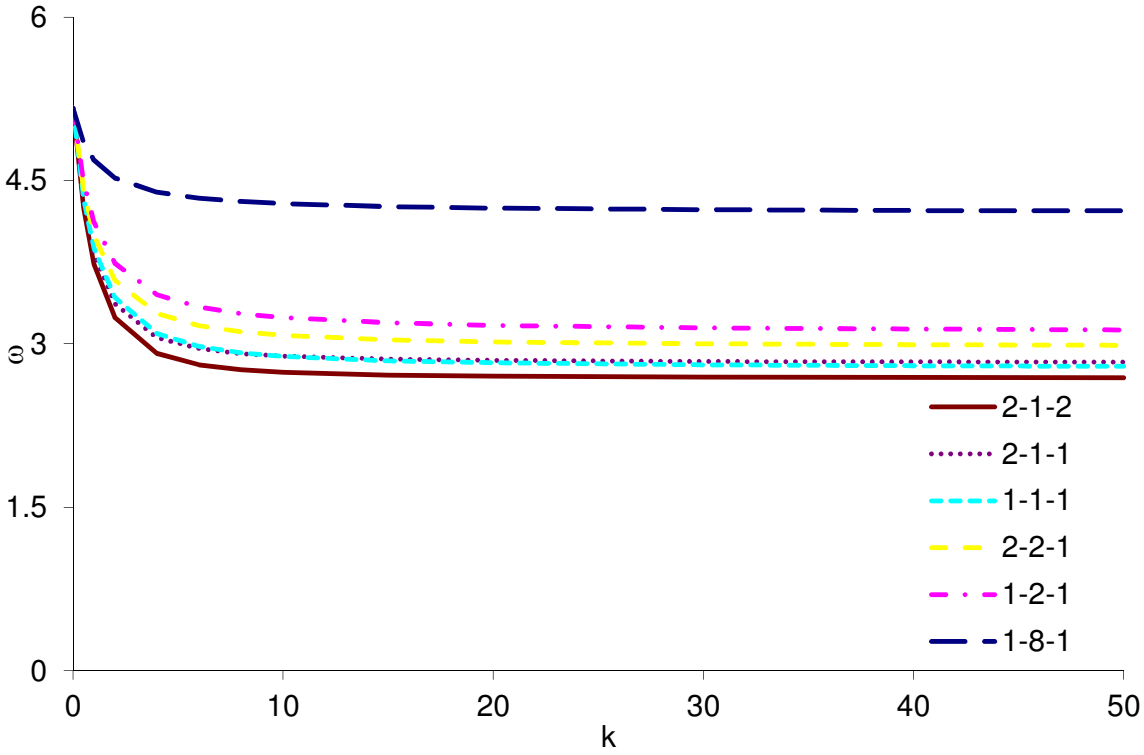

a) Type A

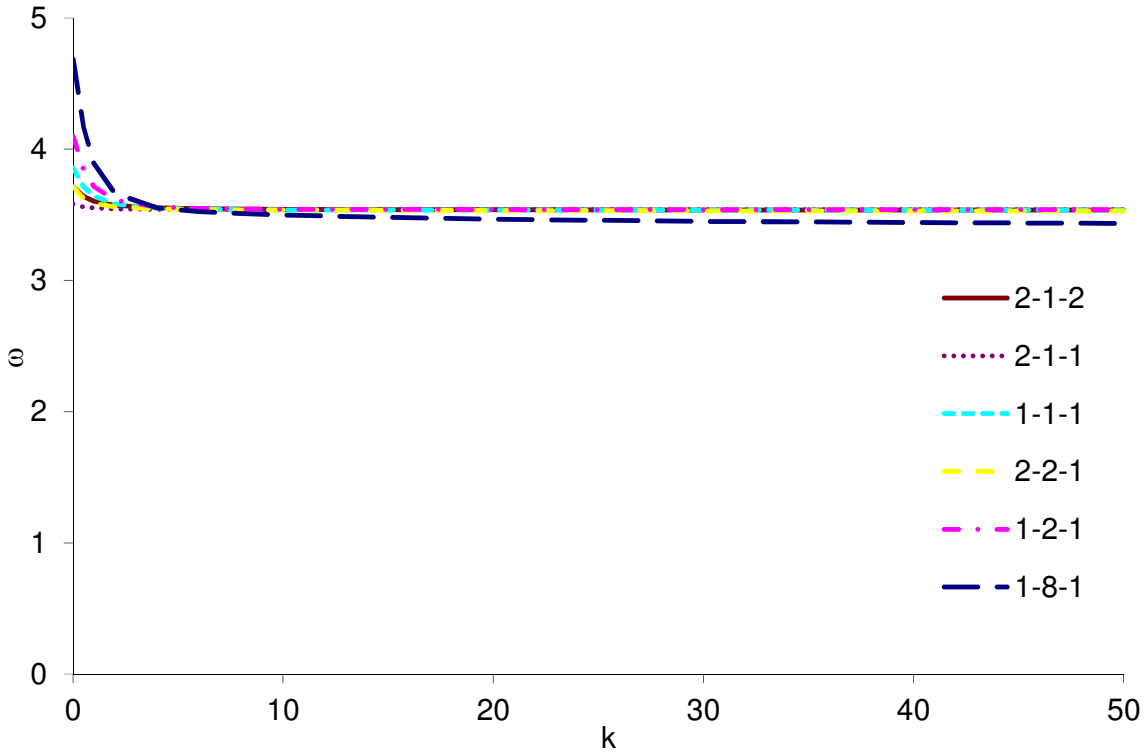

b) Type B

Figure 2: Effect of power-law index k on fundamental frequency obtained from a quasi-3D (HBT, $\varepsilon_z \neq 0$).

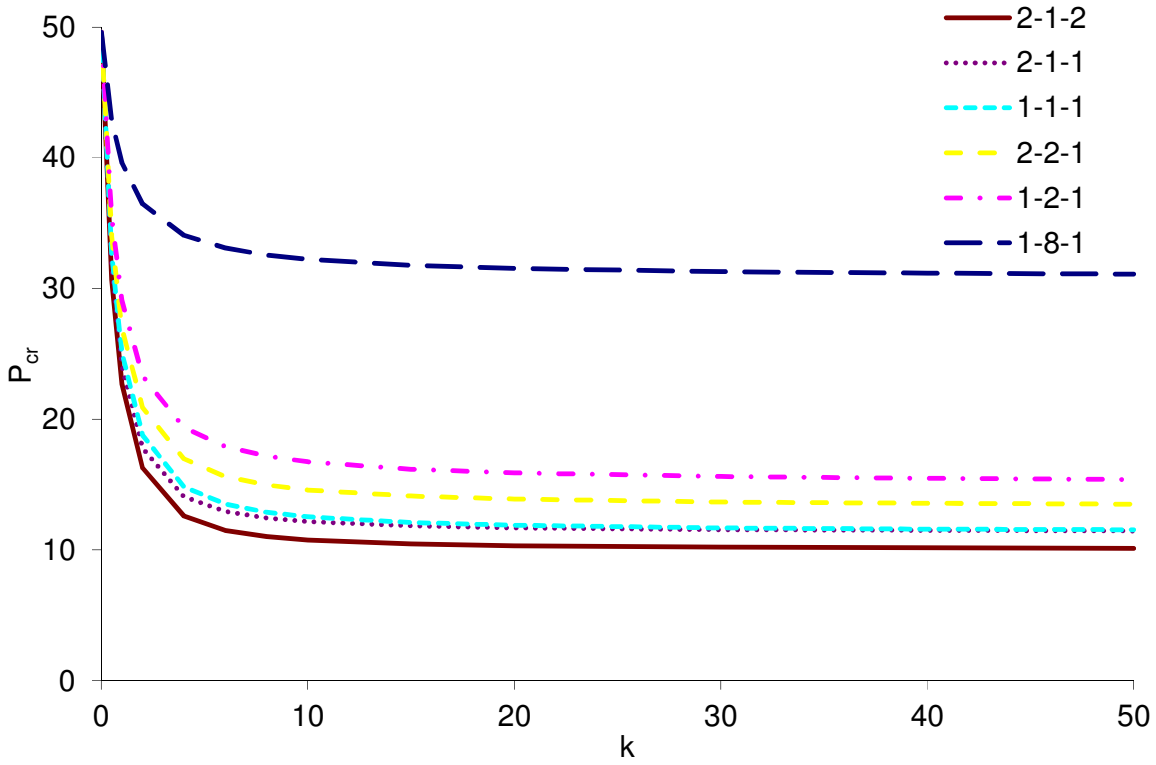

a) Type A

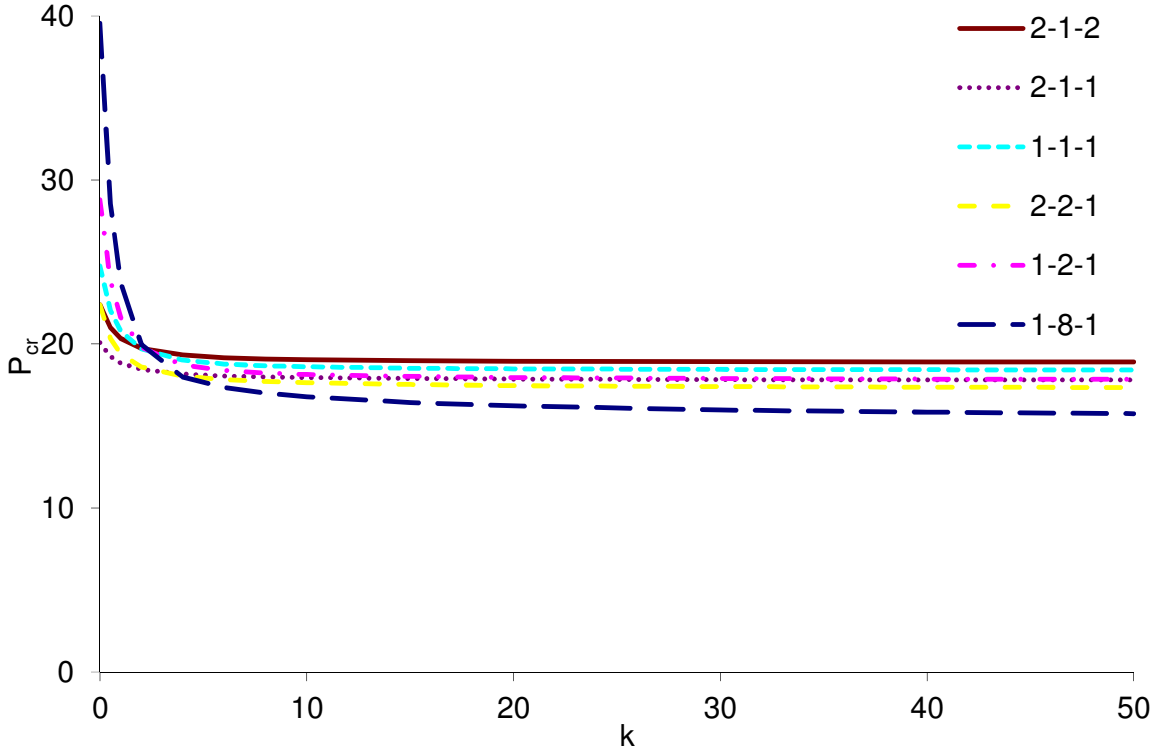

b) Type B

Figure 3: Effect of power-law index k on critical buckling load obtained from a quasi-3D (HBT, $\varepsilon_z \neq 0$).

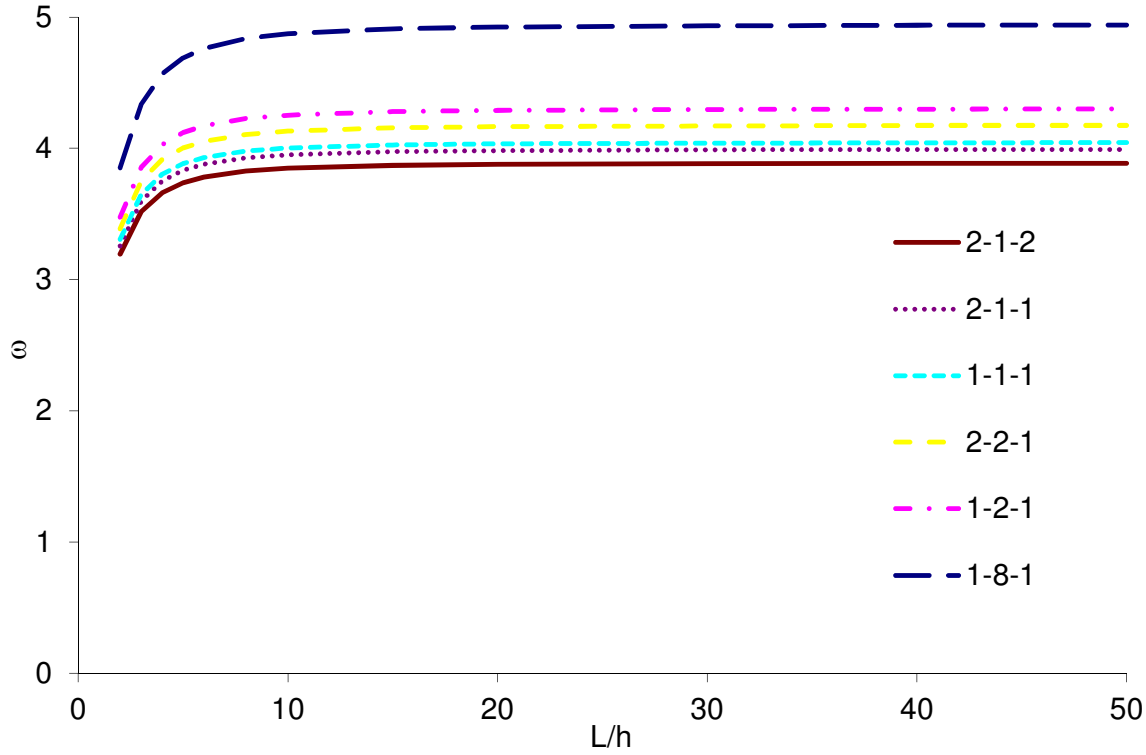

a) Type A

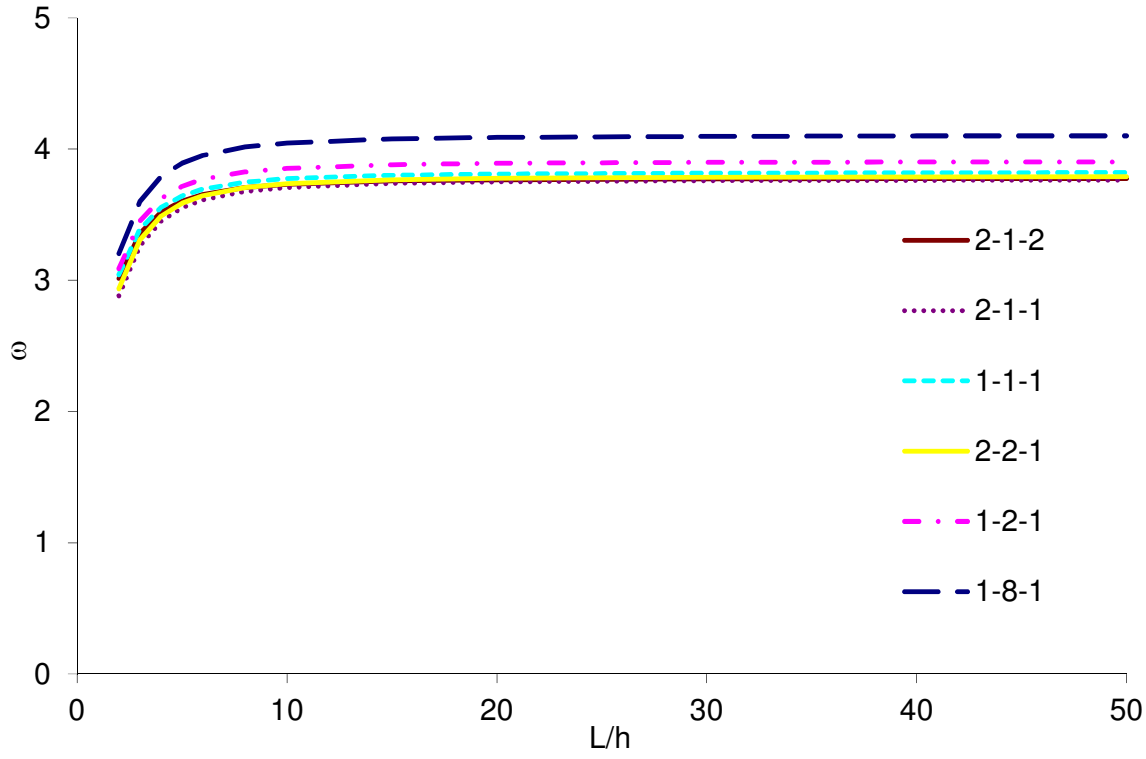

b) Type B

Figure 4: Effect of shear deformation on the fundamental frequency obtained from a quasi-3D (HBT, $\varepsilon_z \neq 0$).

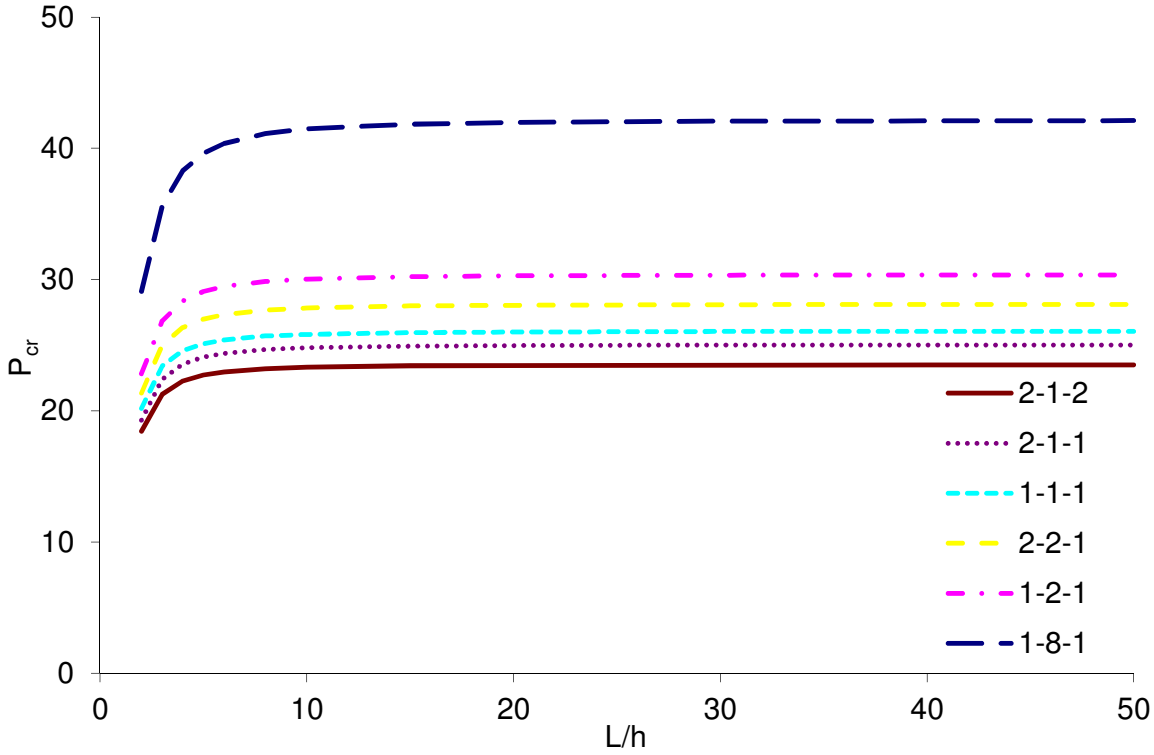

a) Type A

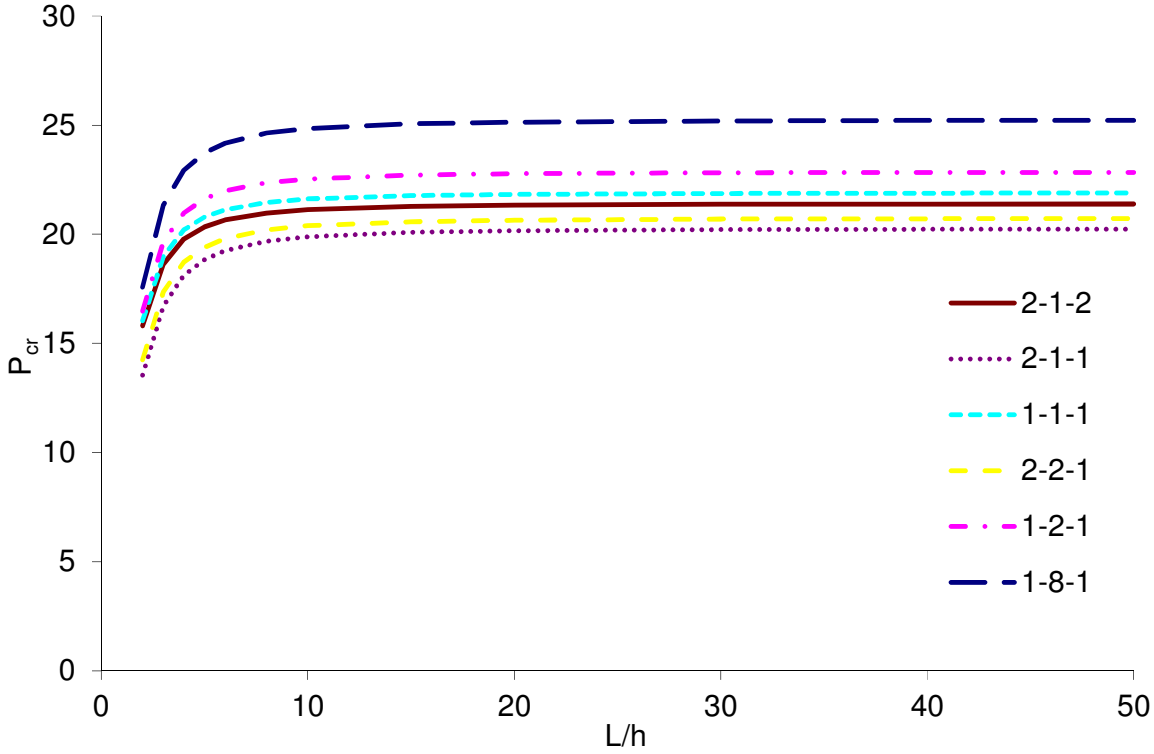

b) Type B

Figure 5: Effect of shear deformation on the critical buckling loads obtained from a quasi-3D (HBT, $\varepsilon_z \neq 0$).

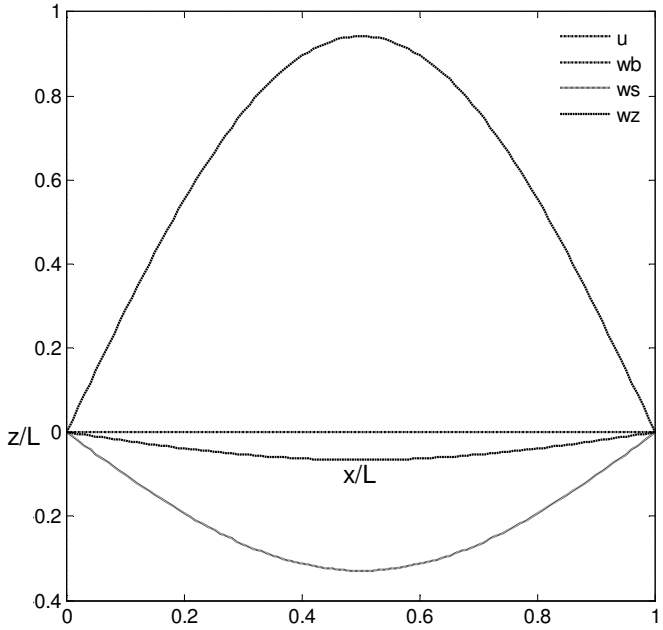

a) First mode $\omega_1 = 4.3588$

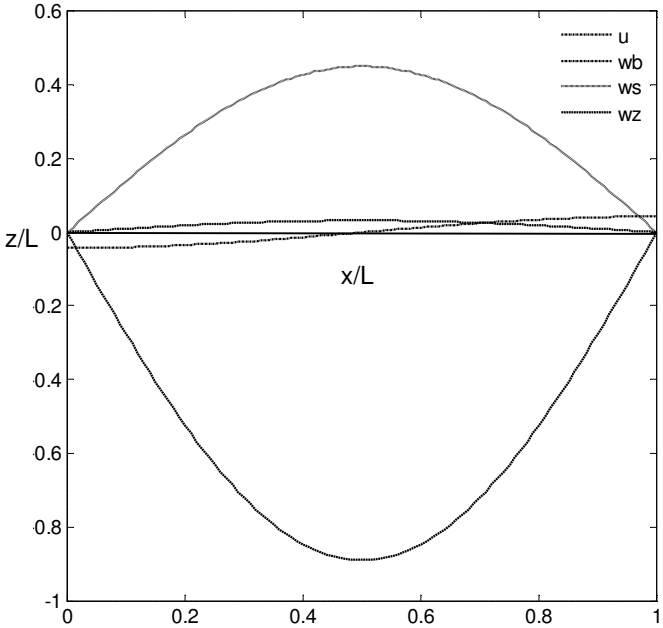

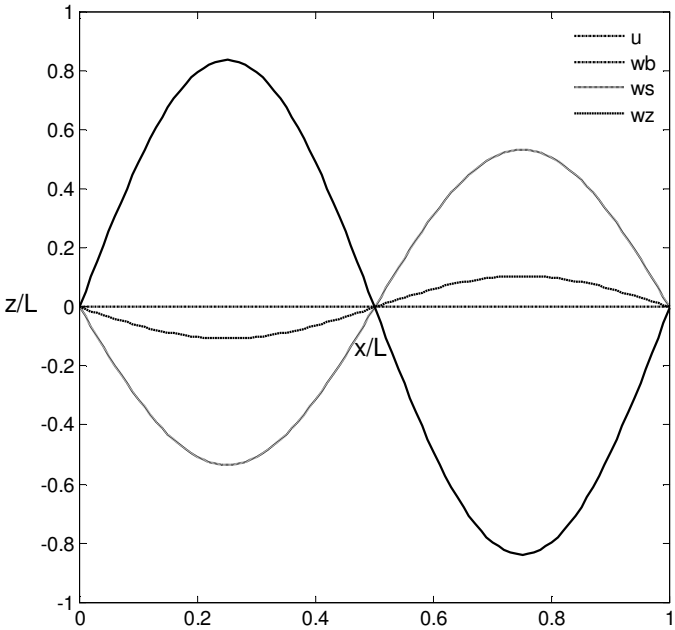

b) Second mode $\omega_2 = 15.5554$

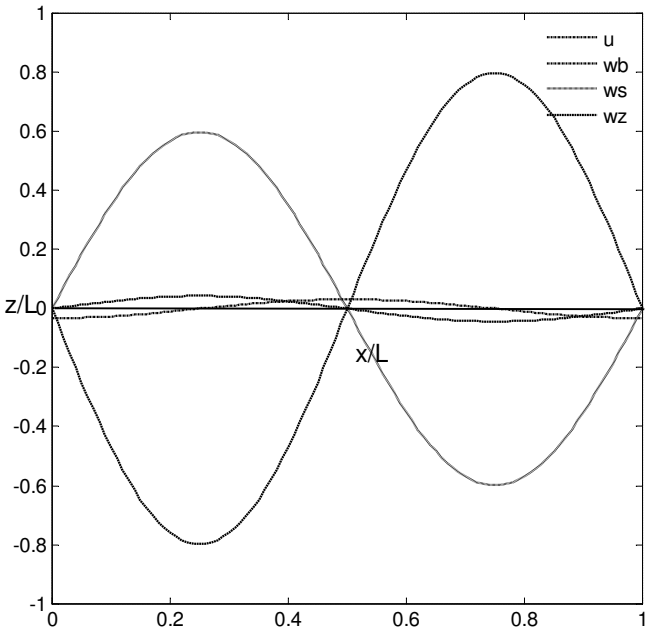

b) Second mode $\omega_2 = 12.0189$

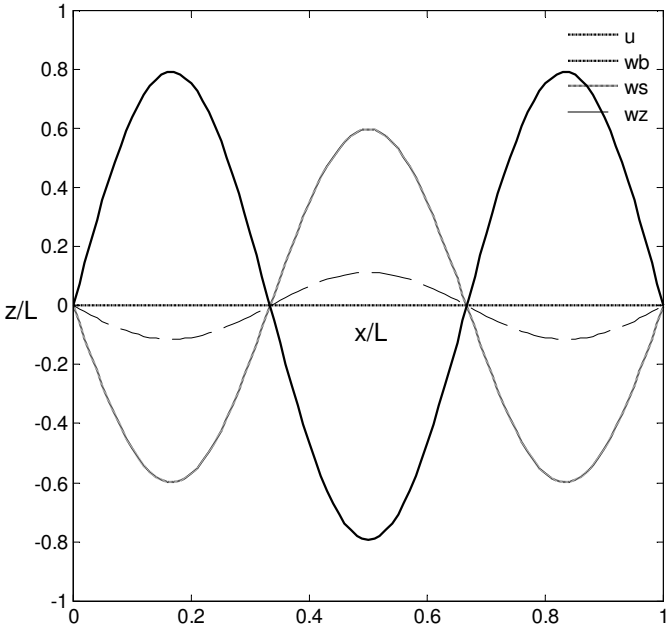

c) Third mode $\omega_3 = 30.4949$

Type A

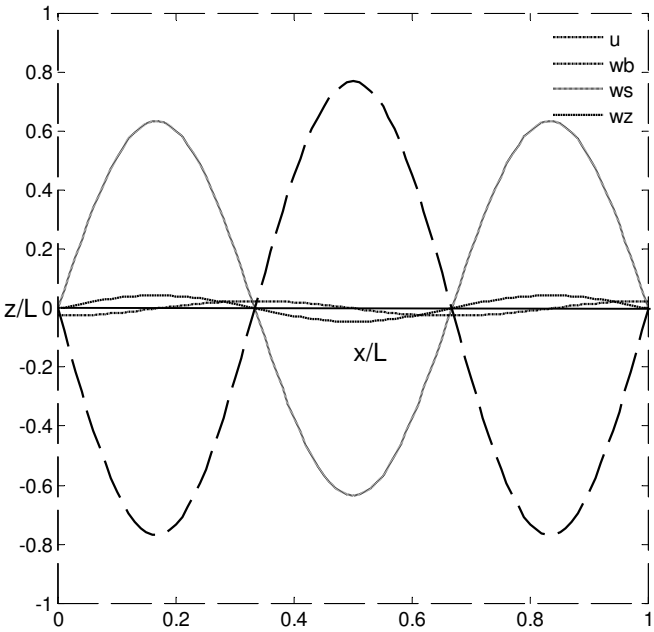

c) Third mode $\omega_3 = 22.6488$

Type B

Figure 6**:** Vibration mode shapes of (1-8-1) sandwich beam (Types A and B, k=5, L/h=5) using a quasi-3D (HBT, $\varepsilon_z \neq 0$).